CONSTRUCTION AND TESTING OF A LOW-TEMPERATURE WATER-GAS SHIFT REACTION SYSTEM

by

Özlem Şen

B. S. in Ch.E., İstanbul University, 2005

Submitted to the Institute for Graduate Studies in
Science and Engineering in partial fulfillment of
the requirements for the degree of
Master of Science

Graduate Program in Chemical Engineering

Boğaziçi University

2008

to my family

ACKNOWLEDGEMENTS

I would like to begin by expressing my truthful gratitude to my thesis supervisor, Prof. Zeynep İlsen Önsan, who has offered continuous encouragement, support and motivation during my MS thesis. Her tremendous amount of guidance has been indispensable for the success of this project. It was a privilege for me to work with Prof. Zeynep İlsen Önsan.

I would also like to acknowledge Assist. Prof. Ahmet Kerim Avcı for providing valuable insights and for his help all the time and Prof. Ayşe Nilgün Akın who has read and commented on my thesis. I am also thankful to Prof. Ahmet Erhan Aksoylu for his support during my thesis.

Very special thanks to my friends Seda Acun, Yasemin Döker and Sadi Tandal Tezcanlı for giving me their everlasting friendship and joyful help.

I also wish to express my great appreciations to all the members of CATREL team, apart from those cited above, Burcu Selen Çağlayan, Şeyma Özkara Aydınoğlu, Feyza Gökaliler for their support, encouragement and friendship.

Cordial thanks for Bilgi Dedeoğlu, Nurettin Bektaş and Yakup Bal for their technical assistance and friendship during my thesis. Heartfelt thanks are for Melike Gürbüz and Fatma Coşkun for their friendship and kindness to me.

Last but not least, I would like to thank my family for their support, patience, encouragement and trust in me throughout my entire education. My father, mother and brother have all been a great source of love for me. Finally, this work is dedicated to them, without whom I am sure that I could not achieve anything.

Financial support provided by Boğaziçi University projects BAP-06HA501 and DPT-07K120630 and by the TÜBİTAK project 104M163 are gratefully acknowledged.

ABSTRACT

CONSTRUCTION AND TESTING OF A LOW-TEMPERATURE WATER-GAS SHIFT REACTION SYSTEM

The objective of this study was to construct and test of a low-temperature water-gas shift reaction system. A system consisting of mass flow controllers for gases, HPLC pump for water, an evaporation and gas-mixing section, a down-flow microreactor located in a temperature-controlled furnace, a water trap, heated stainless steel connecting lines and an on-line gas chromatograph for feed and product analysis was designed and constructed. The testing of the constructed water-gas shift (WGS) reaction system was carried out using three different catalysts prepared by sequential incipient-to-wetness impregnation with fixed platinum and different cerium oxide loadings (1.4wt.%Pt-10wt.%CeO_x/γ-Al_2O_3, 1.4wt.%Pt-5wt.%CeO_x/γ-Al_2O_3, 1.4wt.%Pt-1.25wt.%CeO_x/γ-Al_2O_3). The experimental work involved a parametric study of the effect of catalyst reduction time, reaction temperature, contact time (W/F_{CO}), cerium oxide loading and H_2O/CO ratio on CO conversion. The parametric study was first conducted on 1.4wt.%Pt-10wt.%CeO_x/γ-Al_2O_3 catalyst, except for the H_2O/CO ratio that was tested only on the catalyst with the lowest cerium oxide content. Fresh catalyst samples were reduced *in situ* at 350°C under pure H_2 flow for 2 hours as reduction time had no appreciable effect on CO conversion. W/F_{CO} ratios tested between 0.60-1.25 mg.min.μmol^{-1} indicated that CO conversions increased with increasing contact time. Low-temperature WGS experiments in the 250-350°C interval showed the significant effect of reaction temperature: CO conversion increased with temperature until WGS equilibrium was reached after 300°C and then decreased with the equilibrium curve. CO conversion was the same at CeO_x loadings of 5-10 weight per cent but decreased at 1.25 weight per cent. The effect of H_2O/CO ratio was tested only on 1.4wt.%-1.25wt.%CeO_x/γ-Al_2O_3 for three molar ratios; the results obtained at 250°C showed that CO conversion increased gradually as H_2O/CO ratio reached a value of three.

ÖZET

DÜŞÜK-SICAKLIK SU-GAZI GEÇİŞ REAKSİYONU SİSTEMİNİN KURULMASI VE TEST EDİLMESİ

Bu çalışmanın amacı düşük sıcaklık su-gazı geçiş reaksiyonu sisteminin kurulması ve test edilmesidir. Gazlar için kütle akış kontrol cihazları, su beslemesi için HPLC pompa, buharlaştırma ve gaz karıştırma bölgesi, sıcaklığı kontrol edilen bir fırının içine yerleştirilmiş aşağı-akışlı mikroreaktör, su tutucu, ısıtılmış paslanmaz çelik bağlantı hatları ve besleme ve ürün analizi için gerekli gaz kromatografından oluşan reaksiyon sistemi tasarlanmış ve kurulmuştur. Kurulan su-gazı geçiş reaksiyon sisteminin test edilmesi ardışık emdirme yöntemi ile hazırlanan ve aynı miktarda platin ve farklı miktarlarda seryum oksit içeren üç farklı katalizör (ağırlıkça 1.4%Pt-10%CeO_x/γ-Al_2O_3, 1.4%Pt-5%CeO_x/γ-Al_2O_3, 1.4%Pt-1.25%CeO_x/γ-Al_2O_3) kullanılarak gerçekleştirilmiştir. Deneysel çalışma, katalizör indirgeme süresinin, reaksiyon sıcaklığının, reaktörde kalma süresinin (W/F_{CO}), seryum oksit miktarının ve H_2O/CO oranının CO dönüşmesi üzerine etkisini inceleyen parametrik bir çalışma içermektedir. Sadece en düşük miktarda seryum oksit içeren katalizörde test edilen H_2O/CO oranı dışındaki parametreler, öncelikle ağırlıkça 1.4%Pt-10%CeO_x/γ-Al_2O_3 katalizörü üzerinde incelenmiştir. Taze hazırlanmış katalizöre reaktörde 350^oC sıcaklık ve saf hidrojen akışı altında farklı indirgeme süreleri uygulanmasının CO dönüşmesi üzerinde fark edilir bir değişime neden olmadığı gözlenmiştir. 0.60-1.25 mg.min.μmol^{-1} arasındaki W/F_{CO} oranları, reaktörde kalma süresindeki artmanın CO dönüşmesinde artmaya neden olduğunu; 250-350^oC sıcaklık aralığındaki düşük-sıcaklık su-gazı geçiş deneyleri reaksiyon sıcaklığının CO dönüşmesi üzerinde önemli bir etkisi olduğunu göstermiştir. 300^oC den sonra su-gazı geçiş dengesine erişilene kadar reaksiyon sıcaklığının artması CO dönüşmesini de arttırmış, daha sonra dönüşme oranları denge eğrisine uygun olarak azalmıştır. Ağırlıkça yüzde 5-10 CeO_x içeren katalizörlerde CO dönüşmesi aynı kalmakla birlikte ağırlıkça yüzde 1.25 CeO_x içeren katalizörde azalmıştır. H_2O/CO oranı etkisi sadece ağırlıkça 1.4%Pt-1.25%CeO_x/γ-Al_2O_3 katalizöründe test edilmiş olup, 250^oC sıcaklıkta elde edilen sonuçlar, H_2O/CO oranı üçe ulaştığında CO dönüşümünün de yavaşça artmaya başladığını göstermiştir.

TABLE OF CONTENTS

LIST OF FIGURES

LIST OF TABLES

LIST OF SYMBOLS/ABBREVIATIONS

E_a	Activation Energy
F_{CO}	Carbon monoxide flow rate
ID	Internal diameter
k	Reaction rate constant
K	Numerical value for the equilibrium constant for the reaction
K_i	Adsorption equilibrium constant of component i
MW_i	Molecular weight of component i
OD	Outer diameter
Ox	Oxidized site
P_i	Pressure of component i
r_{CO}	Carbon monoxide consumption rate
R	Universal gas constant
Red	Reduced site
T	Temperature
W_{cat}	Weight of catalyst
W/F_{CO}	Residence time
ΔH_i	Enthalpy of the reaction i at T
ΔGi	Gibbs free energy of reaction i at T
ρ_i	Density of component i
AFC	Alkaline Fuel Cell
ATR	Autothermal Reforming
CH1	Channel 1 setting
CH2	Channel 2 setting
CH4	Channel 3 setting
CNF	Carbon Nanofiber
CP	Co-Precipitation
DMFC	Direct Methanol Fuel Cell

DP	Deposition-Precipitation
FTIR	Fourier Transform Infrared
GC	Gas Chromatograph
GDL	Gas Diffusion Layer
HP	Homogeneous-Precipitation
HPLC	High Performance Liquid Chromatography
HTS	High-Temperature Shift
HT-WGS	High-Temperature Water-Gas Shift
IPOX	Indirect Partial Oxidation
LTS	Low-Temperature Shift
LT-WGS	Low-Temperature Water-Gas Shift
LPG	Liquefied Petroleum Gas
MCFC	Molten Carbonate Fuel Cell
MDP	Modified-Deposition-Precipitation
MEA	Membrane-Electrode Assembly
MMO	Mixed Metal Oxide
PAFC	Phosphoric Acid Fuel Cell
PEMFC	Proton Exchange Membrane Fuel Cell
POX	Partial Oxidation
PROX	Preferential Oxidation
ppm	Parts per million
SOFC	Solid Oxide Fuel Cell
SR	Steam Reforming
TCD	Thermal Conductivity Detector
TOF	Turnover Frequency
UGC	Urea-Gelation Co-Precipitation
WGS	Water-Gas Shift

1. INTRODUCTION

The need for improving the quality of life by developing highly efficient, cleaner and more environmentally friendly energy devices and utilization systems drives the sustainable development of energy systems (Song, 2002). Fuel cells are promising candidates as truly energy-efficient conversion devices (Tabakova *et al.*, 2006). A variety of fuel cells have already been developed, but the proton exchange membrane fuel cells (PEMFC) are being actively considered for automotive applications to lower the fuel consumption and to reduce harmful emissions (Boettner and Moran, 2004). Pure hydrogen is a superior PEMFC feed but its distribution and storage difficulties present serious disadvantages to its direct use for fuel cell propulsion systems (Brown, 2001). Therefore, on-board or *in situ* hydrogen production from a suitable hydrocarbon source appears to be a practical option (Patel and Pant, 2006). Fuel processors can convert most of the available hydrocarbon fuels into hydrogen on-board a vehicle.

In a fuel processor, three catalytic processes are in series for the production of hydrogen: (i) autothermal reforming of hydrocarbon for H_2 production (ATR), (ii) water-gas shift (WGS) reaction and (iii) selective catalytic oxidation of carbon monoxide (PROX). The composition of the gas stream after reforming reactions includes approximately 10 mol per cent carbon monoxide. This CO needs to be removed as it is both a pollutant and a poison for the platinum electrodes of the fuel cell (Goguet *et al.*, 2004). To meet this goal, a WGS converter is added after the reformer to convert CO with water to hydrogen and CO_2. The WGS reaction reduces the CO level to 0.5-1 volume per cent and is generally followed by an additional selective CO oxidation stage to reduce the CO level to about 10 ppm (Zalc *et al.*, 2002).

The WGS is a slightly exothermic and equilibrium limited reaction. Industrially, the WGS reaction is carried out in two stages with different temperature regions. The high-temperature shift (HTS) is at 350-450^{o}C and catalysts are based on Fe-Cr oxides. The low-temperature shift (LTS) is usually between 200-260^{o}C and typical catalysts are based on $Cu/ZnO/Al_2O_3$ (Zalc and Löffler, 2002). Although Cu-based catalysts for low-temperature water-gas shift reaction have long been used, they have strong drawbacks which make

them inappropriate for fuel cells. The low-temperature water-gas shift reaction is also limited by kinetics. Therefore, the development of advanced catalysts is highly demanded. Different metal/support combinations including base (non-precious) metals or noble (precious) metals have been studied. Among those systems, cerium oxide-containing low-temperature water-gas shift catalysts are promising because of the high oxygen storage capacity of ceria and the cooperative effect of ceria-metal leading to highly active sites (Zerva and Philippopoulos, 2006).

Copper-ceria catalysts among the non-precious metal/support systems are the alternatives to the commercial copper-zinc oxide low-temperature water-gas shift catalysts. The preparation method affects the activity of the catalysts directly. Among methods such as impregnation, precipitation, sol-gel and ion-exchange, those more suitable for the preparation of copper-ceria catalysts are precipitation and impregnation (Zerva and Philippopoulos, 2006). The disadvantages of copper-based catalysts have been overcome by the use of precious metal-based systems, although cost is always an important factor. Promotion by a noble metal enhances the reducibility of ceria and assists the formation of surface oxygen vacancies. Au and Pt are the most studied precious metal catalysts for low-temperature WGS reaction. Pt/CeO_2 catalyst seems to be the most promising among those catalysts and is generally prepared by the impregnation method. This catalyst can also be promoted by other metals such as Re, MgO to increase its activity (Farias *et al.*, 2007; Radhakrishnan *et al.*, 2006) while zirconia or alumina can be added to ceria as supports (Zerva and Philippopoulos, 2006). Gold catalysts for low-temperature WGS have also received great attention in recent years. The synthesis of gold catalysts is highly sensitive towards the preparation technique which leads to wide differences in the sizes of gold particles and in their interaction with the support. The precipitation method is the most suitable technique for synthesis of gold-ceria catalysts (Tabakova *et al.*, 2004).

The objective of this study was the construction and testing of an integrated system suitable for studying the low-temperature water-gas shift reaction. After the construction of the reaction system, $Pt\text{-}CeO_x/\gamma\text{-}Al_2O_3$ catalysts were prepared and used to examine the effects of reaction parameters on low-temperature WGS reaction. The catalysts studied were divided into three groups according to their cerium oxide loadings. All of the catalysts were prepared by the sequential impregnation method. The catalytic activity tests

were conducted in a microreactor flow system run at atmospheric pressure at 250, 275, 300 and 350^{o}C. The effects of catalyst reduction time, residence time (W/F_{CO}) and feed composition (H_2O/CO ratio) were also tested.

Section 2 includes a literature survey on fuel cells, on-board hydrogen production, characteristics of high and low-temperature water-gas shift reactions and catalysts used for these reactions, suggested mechanisms and kinetics. Section 3 describes the experimental system constructed and the procedures followed in this study. The details of the reaction system and the results obtained in the experiments are presented and discussed in Section 4, while the conclusions and recommendations for future work are given in Section 5.

2. LITERATURE SURVEY

2.1. Fuel Cells

Currently much attention is focused on fuel cells as a clean and efficient source of electrical power (Wild and Verhaak, 2000). Fuel cell power generation is undergoing rapid development both for stationary and transportation applications. In the transportation sector, fuel cells could replace the internal combustion engines in cars, trucks, buses, etc. while meeting the most stringent emission regulations. Their thermodynamic efficiency is in fact generally much higher than that of thermal engines. Although other factors limit the efficiency of the present-generation fuel cells to 40-50 per cent, it is still two to three times that of the internal combustion engine of a typical vehicle (Li *et al*., 2000).

Fuel cells are devices that convert energy into electrical energy without involving combustion cycles. Oxygen and a fuel obtainable from gasoline, natural gas or methanol are fed to the electrodes and chemical energy is directly converted into electricity. Heat and water vapor are the only by-products (Li *et al.*, 2000; Alcaide *et al.*, 2006).

Different reactions occur in a fuel cell depending on the electrode type and fuel. The electrochemical process taking place in the fuel cell is clean, quiet and highly efficient. Fuel cells are characterized by their operation temperature and their electrolytes. These different types of fuel cells are:

- Proton exchange (or polymer electrolyte) membrane fuel cells (PEMFC)
- Phosphoric acid fuel cells (PAFC)
- Alkaline fuel cells (AFC)
- Direct methanol fuel cells (DMFC)
- Molten carbonate fuel cells (MCFC)
- Solid oxide fuel cells (SOFC)
- Regenerative fuel cells

According to the operation temperature, there are two major types of fuel cells: low temperature and high temperature fuel cells. Proton exchange membrane, phosphoric acid, alkaline and direct methanol fuel cells operate at low temperatures. In contrast, the molten carbonate and solid oxide fuel cells operate at high temperatures. They are suitable for stationary rather than vehicular applications because of their high operating temperature. The electrolytes can be aqueous, molten or solid. In the low temperature fuel cells, the aqueous electrolytes are used. The molten electrolytes are usually employed at high temperatures and the solid electrolytes at quite higher temperatures (Alcaide *et al.*, 2006). Phosphoric acid fuel cells, molten carbonate fuel cells and solid oxide fuel cells are being used for central power plant applications due to their high power generation and durability (Son, 2006).

The most promising fuel cell technology for transportation applications appears to be the polymer electrolyte membrane fuel cell (PEMFC) (Trimm and Onsan, 2001). Polymer electrolyte fuel cells (PEMFCs) fueled by hydrogen have been extensively studied due to their attractive properties, such as high power density, low emissions (NO_x, dust, noise), low temperature operation, low weight, compactness, potential for low cost and volume, long stack life, fast start-ups and suitability to discontinuous operation (Scherer, 1997; Ahmed and Krumpelt, 2001; Ghenciu, 2002).

In a PEMFC, hydrogen gas is electrocatalytically oxidized to hydrogen ions (Reaction 2.1) at the anode electrocatalyst that is composed of Pt deposited on a conductive carbon. The cell operates at approximately 70-80^{o}C. The protons released during the oxidation of hydrogen are conducted through the proton exchange-membrane to the cathode. The cathode is comprised of Pt on carbon and electrocatalytically reduces oxygen in the air to combine with the protons and thereby, produce water and heat (Reaction 2.2). Therefore the overall reaction can be expressed as follows (Reaction 2.3):

$$H_2 \rightarrow 2H^+ + 2e^- \text{ (anode)} \quad (2.1)$$

$$½\ O_2 + 2H^+ + 2e^- \rightarrow H_2O \text{ (cathode)} \quad (2.2)$$

$$H_2 + ½\ O_2 \rightarrow H_2O \text{ (overall)} \quad (2.3)$$

The heart of the PEMFC is the membrane-electrode assembly (MEA). The MEA consists of a proton exchange membrane (poly-perfluorosulfonic acid, Nafion), the catalyst layers of both electrodes and gas-diffusion layers (GDLs) that are constructed from porous carbon paper or carbon cloth. These components are then pressed together at high temperature and pressure (Litster and McLean, 2004).

Carbon monoxide present in the fuel gas deteriorates the Pt electrode of PEMFC and degrades the cell performance and it is known as CO poisoning (Iida and Igarashi, 2006). The CO competes with the adsorption of hydrogen on the active sites of platinum at normal anode operating potentials. CO reacts with the hydroxyl species that are adsorbed on the platinum surface to form CO_2. This case results, however, in a serious loss of efficiency and is not practical (Adams *et al.*, 2005).

In the proton exchange membrane fuel cells, hydrogen is used as a fuel. However, use of H_2-PEMFC in vehicles is associated with considerable problems as far as the storage and distribution of hydrogen are concerned (Goerke *et al.*, 2004). Hydrogen can be stored in pressurized vessels or metal hydrides. However, these systems occupy space in a vehicle, increase weight and decrease fuel efficiency. The storage of hydrogen in carbon nanotubes offers a feasible alternative, but the production and distribution of the gas remains as a difficulty (Trimm and Önsan, 2001).

Therefore a promising method to overcome the problem of storage and the distribution infrastructure and also non-existing large scale hydrogen production is to produce hydrogen on-board (Kusar *et al.*, 2006). The integration of fuel cells with compact and efficient fuel processors which convert available hydrocarbon fuels into hydrogen on-board is therefore considered (Avcı *et al.*, 2003).

2.2. On-Board Hydrogen Production

In the hydrogen production process, the efficient operation of a fuel processor is mostly based on the successful selection of fuel, fuel conversion mechanism and catalyst combinations (Avcı *et al.*, 2003).

There are different fuels for on-board hydrogen production. Natural gas, liquefied petroleum gas (LPG), gasoline, diesel or methanol are attractive alternatives. Diesel deposits coke too easily and is not suitable but conversion of the other fuels is possible (Avcı *et al.*, 2001).

PEMFC operation requires the continuous availability of hydrogen. Hence, attention has been focused on the conversion of more readily available hydrocarbon fuels to hydrogen. Natural gas is an available option since the transportation and storage are not the problems. Natural gas is mainly composed of methane; the number of hydrogen atoms per carbon atom is close to 4:1, which is greater than those of higher hydrocarbon fuels such as LPG and gasoline (Avcı *et al.*, 2002).

The conversion of hydrocarbon fuels to hydrogen in a fuel processor can be carried out by several reaction processes, including steam reforming (SR), partial oxidation (POX) and autothermal reforming (ATR) (Krumpelt *et al.*, 2002). Nearly all processes considered for commercial exploitation are based on autothermal reforming where without water it is partial oxidation (POX) and without oxygen it is steam reforming (SR) and autothermal reforming of a hydrocarbon is the first step of the hydrogen production process (Trimm and Önsan, 2001; Son and Lane, 2001). In general autothermal reforming has a better capacity for start-up than steam reforming, because the unit can be quickly brought up to desired operating temperature by running in combustion mode for a short time (Zalc and Löffler, 2002).

In the steam reforming, steam reacts with the fuel in the presence of a catalyst to produce hydrogen, carbon monoxide and carbon dioxide. Steam reforming may be applied both to alcohols and to hydrocarbons.

Steam reforming of alcohols;

$$CH_3OH + H_2O \leftrightarrow CO_2 + 3H_2 \qquad (2.4)$$

Steam reforming of hydrocarbons;

$$CH_4 + H_2O \leftrightarrow CO + 3H_2 \qquad (2.5)$$

The reaction is strongly endothermic and heat must be supplied to the system. This is usually done by combusting part of the fuel (Trimm and Önsan, 2001):

$$CH_4 + 2O_2 \leftrightarrow CO_2 + 2H_2O \quad (2.6)$$

Partial oxidation (POX) and indirect partial oxidation (IPOX) –which is the combination of total oxidation and steam reforming reactions-, are accepted to be the most promising routes to produce hydrogen from hydrocarbon fuels for mobile applications.

Autothermal reformers combine the heat effects of the endothermic steam reforming (SR) and exothermic partial oxidation (POX) reactions by feeding the fuel, water and dry air together into the reactor: (fuel + air + steam→ carbon oxides + hydrogen). This process is carried out in the presence of a catalyst, which controls the reaction pathways and thereby determines the relative extents of the oxidation and steam reforming reactions (Ahmed and Krumpelt, 2001). The products from these reactions include CO and it presents problems, because Pt electrode on PEMFC is not tolerant to fuels containing CO more than 20 ppm (Jacobs e*t al.*, 2004). It is necessary to achieve low levels of CO by removal from reformed gas.

The water-gas shift (WGS) reaction, the second step in the hydrogen production following autothermal reforming, eliminates most of the CO and produces more hydrogen. The gas from the reformer and water-gas shift reactor contains H_2, CO_2, H_2O, traces of unconverted fuel and 0.5-1 volume per cent CO (Sedmak *et al.*, 2004). It is imperative to lower the remaining carbon monoxide at the third and final cleanup step by preferential oxidation (PROX). The PROX reaction is the selective catalytic oxidation of CO ($CO + ½ O_2 \rightarrow CO_2$). In order to achieve low CO concentration, the PROX reactor is placed between the shift reactor and the fuel cell anode (Cheekatamarla *et al.*, 2005). Selectivity is a serious issue in the PROX unit, because the oxidation of hydrogen leads to diminished process efficiency and increased water management issues. Therefore, the reforming, water-gas shift and preferential oxidation reactors represent a large fraction of the volume and cost and pose the greatest technical challenges (Zalc and Löffler, 2002).

2.3. Water-Gas Shift Reaction

The water-gas shift (WGS) is an old and a key reaction in the production of hydrogen for proton exchange membrane fuel cells (PEMFCs). It is an integral part of fuel processing (Kim and Thompson, 2005; Fu *et al.*, 2005). In a fuel processor for a 50 kW automotive system, a steam or autothermal reformer would generate around 50-60 mol per cent hydrogen, accompanied by roughly 10 mol per cent carbon monoxide, with the balance primarily composed of carbon dioxide, steam, nitrogen and unconverted fuel (Brown, 2001; Docter and Lamm, 1999; Basini and Piovesan, 1998). The WGS process provides a means of utilizing most of the CO by reaction of a gas mixture of CO and H_2O to obtain hydrogen and carbon dioxide. The reaction is reversible and the forward rate is strongly inhibited by the reaction products.

$$CO + H_2O \leftrightarrow H_2 + CO_2 \qquad (2.7)$$

where ΔH= -41.2 kJ.mol^{-1} and ΔG= -28.6 kJ.mol^{-1} (Wen *et al.*, 2007; and Li *et al.*, 2000). WGS units are placed downstream of the reformer to further lower the CO content and improve the H_2 yield and H_2 produced is a very effective reductant for NO_x removal (Ghenciu, 2002; Idakiev *et al.*, 2004). This primary CO clean-up step is essential to adjust the CO:H_2 ratio to the desired value and it reduces the concentration of CO to 0.5-1 volume per cent (5000-10000 ppm) prior to selective CO oxidation (Trimm, 2005).

The WGS reaction is moderately exothermic and equilibrium limited. The equilibrium conversion of CO is dependent largely on the reaction temperature: since the shift reaction is an exothermic reaction, lower temperature is favored for higher CO removal. On the other hand, from the view point of kinetics, the reactant gases are not active enough to reach the chemical equilibrium at low temperature. Favorable kinetics can be achieved at higher temperatures. Therefore, there should be an optimum temperature for WGS reaction. Thermodynamics mandates that the optimum temperature is between 200 and 280^{o}C to achieve desired conversion levels. In addition, CO_2 in the reformed gases suppresses WGS reaction according to Le Chatelier's principle (Shishido *et al.*, 2006a; Tanaka *et al.*, 2003b).

Existing industrial applications of WGS reaction typically combine a high-temperature shift (HTS) stage and a low-temperature shift (LTS) stage on the basis of thermodynamic considerations.

2.3.1. High-Temperature Water-Gas Shift Reaction

The high-temperature shift (HTS) reactor operates at 350-450^{o}C and provides the fast reaction kinetics. The CO concentration is reduced to about three-five volume per cent by high-temperature water-gas shift (HT-WGS) reaction. Conventional HT-WGS catalysts are based on iron-chromium (Fe-Cr) oxides and they have some advantages such as, low cost, long life and are reasonably resistant to sulfur, but they are inactive at temperatures below about 300^{o}C (Kumar and Idem, 2007; Trimm, 2005).

This type of catalyst has demonstrated high WGS activity and excellent thermo-stability, probably because the iron oxide is structurally promoted by the chromium oxide and the chromium promoter acts as a structural stabilizer. In the absence of chromium oxide, the effective lifetime of the catalyst is severely restricted due to rapid thermal sintering. Although Fe-Cr catalysts have been widely used in the HTS reaction, the role of the Cr_2O_3 addition on the stabilization of the catalyst structure is still unclear. However, it has been proposed that chromia forms a solid solution in Fe_3O_4 and that Cr^{3+} displaces equal amounts of Fe^{2+} and Fe^{3+} from the octahedral sites and the displaced Fe^{2+} is consequently located in the tetrahedral site (Rhodes *et al.*, 2002; Natesakhawat *et al.*, 2006).

Conventional HT-WGS catalysts based on oxides of iron chromium are well established industrially, but further promotion is desirable. There have been some studies on the addition of a range of materials as promoters for the Fe_3O_4/Cr_2O_3 catalyst. The promotion of the catalyst by the addition of small amounts of metal can be advantageous. A series of Fe_3O_4/Cr_2O_3 catalysts containing two weight per cent B, Pb, Cu, Ba, Ag and Hg were prepared and tested for the WGS reaction at the temperature range 350-440^{o}C. The order of activity across the temperature range was found to be Hg>Ag, Ba>Cu>Pb>B. The addition of boron does not significantly affect the activation energy, but the addition of Pb, Cu, Ba, Ag, Hg all decreases the activation energy markedly under these conditions.

However, it should also be noted that, in this study, the effect of these additives on catalyst lifetime has not been investigated and, consequently, it is not possible to comment on the stability of Ag^{+}, Ba^{2+} and Hg^{2+} as promoters (Rhodes *et al.*, 2002).

Iron-chromium oxides can be promoted with precious metals as well as base metals. Lei *et al.* (2005a) investigated the promotional effect of Rh, Pt, Pd. It was found that the promotional trend for WGS was Rh>Pt>Pd. Rh/Cr_2O_3-FeO_4 is the most active catalyst; the rate at 350^{o}C is almost twice that of the next most active. Also the rhodium promotion accelerates the Fe_3O_4 (magnetite) formation from Fe_2O_3 (hematite). Fe_3O_4 is the stable oxide in equilibrium with WGS feeds (Lei *et al*., 2006).

$$3Fe_2O_3 + H_2 \rightarrow 2Fe_3O_4 + H_2O \qquad (2.8)$$

The rhodium promoted sample is almost five times more active as the unpromoted one at 350^{o}C and 1.5 times more active at 500^{o}C. The rate advantage over the commercial HT-WGS catalyst is slightly greater (Lei *et al.*, 2006).

The commercial iron-based WGS catalysts with as high as 8-14 weight per cent Cr promoter generally contain about two weight per cent Cr^{6+} compound. The use of chromium poses additional complications due to harmful effects of Cr^{6+} on human health and environment (Liu *et al.*, 2005a; Natesakhawat *et al.*, 2006). Therefore, the search for less toxic catalysts can be taken into consideration. Chromium can be replaced by other catalysts meeting the requirements of the function of it.

The thorium- and copper-doped magnetite is a promising option to replace the chromium- and copper-doped catalyst. In thorium- and copper-doped magnetite, copper acts as a structural promoter whereas thorium prevents sintering and the production of metallic iron which can catalyze undesirable reactions. However, thorium damages some active sites and decreases the activity per area. The most active catalyst is obtained when both thorium and copper are present in the solid. This catalyst is more active and selective than a chromium- and copper-doped commercial one and it shows several important features like be non-toxic, in comparison to the high chromium toxicity (Costa *et al.*, 2002).

Aluminum is another convenient option to replace chromium in copper-based HTS catalysts. The addition of small amounts of copper to aluminum-doped hematite leads to better catalytic properties. Likely, copper behaves as a structural promoter while aluminum is a textural one. This sample easily produces the active phase, but it is resistant to further magnetite reduction. This catalyst has similar catalytic properties, as compared to the chromium and copper-doped commercial one and it can also work at energy saving conditions. However, it has the advantage of being discarded without any damage to the environment (Araujo and Rangel, 2000).

The chromium-free iron catalyst is also a good alternative to traditional Fe-Cr WGS catalysts. This chromium-free iron catalyst can be promoted by oxides of Ce and Al. Iron in the fresh chromium-free catalyst is presented as γ-Fe_2O_3. During reduction and reaction, most of the γ-Fe_2O_3 in the catalyst is transformed to the Fe_3O_4 with perfect structure. It is postulated that Fe_3O_4 acts as active phase for WGS reaction (Liu *et al.*, 2005a). Also the addition of aluminum stabilizes the magnetite phase by retarding its further reduction to FeO or metallic iron (Natesakhawat *et al.*, 2006).

If metallic iron is formed, methanation or CO disproportionation may occur. Methanation is a problem generally associated with HT-WGS reaction. It can reduce the hydrogen yield and can also increase the temperature of the catalyst due to exothermic reaction leading to catalyst deactivation, thereby lowering the efficiency of hydrogen production.

$$3H_2 + CO \leftrightarrow CH_4 + H_2O \qquad (2.9)$$

where $\Delta H = -205.8$ kJ.mol^{-1} (Kumar and Idem, 2007; Kusar *et al.*, 2006).

2.3.1.1. High-Temperature Water-Gas Shift Reaction Mechanism and Kinetics. Although the WGS reaction has only four small molecules, the reaction mechanism is quite complex and there is still some discussion about it (Koryabkina *et al.*, 2003). There are several mechanisms for the HT-WGS reaction.

In the adsorptive mechanism, the reaction proceeds via the formation of an adsorbed formate group which decomposes to hydrogen and carbon dioxide.

(i) $H_2O + 2* \rightarrow HO* + H*$ (2.10)

(ii) $CO + * \rightarrow CO*$ (2.11)

(iii) $CO* + HO* \rightarrow *\text{-}O\text{-}CH{=}O$ (2.12)

(iv) $*\text{-}O\text{-}CH{=}O \rightarrow CO_2 + H*$ (2.13)

(v) $2H* \rightarrow H_2 + *$ (2.14)

where "*" represents a surface vacancy. This is one of the mechanisms by which the increased activity of the copper-doped catalysts can be explained. The reactants adsorb on the catalyst surface, where they react to form surface intermediates, such as formates, followed by decomposition to products and desorption from the surface (Trimm, 2005; Costa *et al.*, 2002).

In the regenerative (oxidation-reduction) mechanism of the copper-doped catalysts, the surface undergoes successive oxidation and reduction cycles by water and carbon monoxide, respectively, to form the corresponding hydrogen and carbon dioxide products.

(i) $CO + * \rightarrow CO*$ (2.15)

(ii) $H_2O + MO \rightarrow H_2 + MO_2$ (2.16)

(iii) $MO_2 + CO \rightarrow CO_2 + MO + *$ (2.17)

It is proposed that the redox regenerative mechanism is a dominant pathway for the WGS reaction on the chromium-free iron catalyst (Liu *et al.*, 2005a). Iron-chromium oxide WGS catalysts appear to operate by a mechanism that includes adsorptive and redox steps, for example,

(i) $CO + O\ (s) \rightarrow CO_2\ (s)$ (2.18)

(ii) $CO_2\ (s) \rightarrow CO_2 + *$ (2.19)

(ii) $H_2O + * \rightarrow H_2O\ (s)$ (2.20)

(iii) $H_2O\ (s) + O\ (s) \rightarrow 2OH\ (s)$ (2.21)

(iv) $2OH\ (s) \rightarrow 2O\ (s) + H_2$ (2.22)

where (s) represents a surface species. The first step (reduction by CO) or the final step (hydrogen release) can be rate-limiting in the HT-WGS reaction catalyzed by Rh-promoted Fe_3O_4-Cr_2O_3 catalysts (Lei *et al.*, 2006).

The kinetics of the HT-WGS reaction have been studied extensively and the reaction models are based either on a Langmuir-Hinshelwood approach:

$$r = \frac{kK_{CO}\ K_{H_2O}\left[[CO]\ [H_2O] - [CO_2]\ [H_2]/K\right]}{\left(1 + K_{CO}[CO] + K_{H_2O}[H_2O] + K_{CO_2}[CO_2] + K_{H_2}[H_2]\right)^2} \tag{2.23}$$

where k is the rate constant, K_i the adsorption equilibrium constant of species i at concentration [i] and K is the numerical value for the equilibrium constant for the WGS reaction, or on a power rate law basis with rate expressed as either

$$rate = k[CO]^m[H_2O]^n[CO_2]^p[H_2]^q \tag{2.24}$$

or

$$rate = k_1[CO]^a[H_2O]^b[CO_2]^c[H_2]^d(1-\beta) \tag{2.25}$$

$$\beta = \frac{[CO_2]\ [H_2]}{K[CO]\ [H_2O]} \tag{2.26}$$

The power rate law model was found to be sufficient for most reactor design studies (Lei *et al.*, 2005b).

2.3.2. Low-Temperature Water-Gas Shift Reaction

The low-temperature shift (LTS) reactor operates at temperatures between 200 and 260^{o}C to take the advantage of the shift of the equilibrium to lower CO concentrations at lower temperatures (Leppelt *et al.*, 2006). The CO concentration is further reduced to about 0.5-1 volume per cent with low-temperature water-gas shift reaction.

In fuel processors, the low-temperature water-gas shift (LT-WGS) reactor is generally placed after the autothermal reformer (ATR) where some HT-WGS also occurs. A separate HT-WGS reactor may not be required in the process, because water is used with CO as inlet stream and this provides energy integration which reduces the temperature to low-temperature shift ranges (Avcı *et al.*, 2002). Commercial WGS formulations occupy ca. 30-50 per cent of the catalyst volume and weight of the fuel processor. Most of this volume is the LT-WGS reactor which takes a considerable part of the overall fuel processor due to the low operating temperatures resulting in slow kinetics (Ghenciu, 2002; Quiney *et al.*, 2006).

The commercial catalysts used in LT-WGS process usually consists of different combinations of CuO, ZnO and Al_2O_3 components. The copper and zinc oxide forms are stable under reaction conditions. Unfortunately, these catalysts are extremely pyrophoric in activated (reduced) state and may cause explosion upon exposure to air, which makes them impossible to use in automobile and several other applications (Ruettinger *et al.*, 2003). These catalysts are very sensitive to temperature excursions, therefore they have narrow operating temperature window. They are also very susceptible to shut-down and start-up cycling because the active component of the catalyst is leached out by condensed water during quenching or deactivated by the formation of surface carbonates. These catalysts require careful preactivation in H_2. Control of temperature is essential during activation, since the reduction of the catalyst is highly exothermic. As a result, these $Cu/ZnO/Al_2O_3$ catalysts are more suitable for service stations applications than for mobile use (Kusar *et al.*, 2006; Trimm, 2005).

The design of LT-WGS catalysts to be used for fuel processors must address the above mentioned deficiencies. Amongst the requirements imposed on LT-WGS catalysts for use in fuel processors are: high activity at relatively low temperature, stability under typical reformate outlet to insure low, steady outlet CO concentration within minimal catalyst volume, non-pyrophoric formulations in order to eliminate pre-conditioning steps, durability under steady state and transient conditions, mechanical integrity under temperature excursions, stability to condensation and to poisons such H_2S, chlorine. Also these catalysts should demonstrate high selectivity imposed by a range of H_2O/CO ratios, with no side reactions. The resistance of these catalysts to the adverse effects of potential

hydrocarbons from the upstream reformate is among the important properties that they should have (Ghenciu, 2002).

2.3.2.1. Non-Precious (Base) Metal Catalysts. Non-precious metal formulations for LT-WGS are sought based on their low cost compared to precious metal catalysts.

Among the non-precious metal catalysts, copper-based catalysts are generally more active for LT-WGS. Though copper-based catalysts have been the subject of extensive studies for the water-gas shift reaction ever since they were introduced in the early 1960s, some important aspects of the reaction over these catalysts have not yet been addressed properly. For example, the nature of sites for copper-based shift catalysts is a topic of controversy (Yeragi *et al.*, 2006). Some studies indicate that metallic copper is the active phase for reaction (Koryabkina *et al.*, 2003). Also the activity of the copper-based catalysts can be affected by the preparation method and pretreatments such as calcination and reduction.

Ternary $Cu/ZnO/Al_2O_3$ catalyst has been widely employed commercially in the LT-WGS reaction and this catalyst is usually prepared by co-precipitation (CP) method to afford the higher Cu metal dispersion in the resulting catalyst and, as a consequence, the higher catalytic activity. In the study of Shishido *et al.* (2006a) binary Cu/ZnO and ternary $Cu/ZnO/Al_2O_3$ catalysts were prepared by homogeneous precipitation (HP) by urea hydrolysis. It is expected that the homogeneity of the precipitate obtained by this method will be higher than that prepared by CP, since there is no gradient in concentration of precipitants in the solution. The catalysts prepared by both CP and HP contained apparently CuO and ZnO as crystalline phase in both catalysts; the amount of Al was small as 10 at. per cent in the ternary catalysts. Homogeneous precipitation (HP) afforded high activity as well as sustainability to both Cu/ZnO and $Cu/ZnO/Al_2O_3$ catalysts, among which the binary catalysts showed higher activity than the ternary catalysts. Binary HP-Cu/ZnO showed higher activity than ternary $Cu/ZnO/Al_2O_3$, even though the surface area was larger on the latter than on the former. The activity apparently depended on the surface area of Cu metal formed on the surface of HP-catalysts and a good correlation was observed between the Cu metal particle size and the activation energy of the shift reaction.

The commercial $Cu/ZnO/Al_2O_3$ catalyst can also be prepared by impregnation. The catalytic activity of the impregnated catalyst is comparable that of prepared by co-precipitation (CP) at temperatures above 200^oC. The optimum composition of the impregnated catalyst for high WGS reaction activity is five weight per cent Cu/five weight per cent ZnO/Al_2O_3 and smaller than that of co-precipitated catalyst. However, the activity of the impregnated $Cu/ZnO/Al_2O_3$ catalysts is significantly lowered at 150^oC, whereas no deactivation is observed for the co-precipitated catalyst at the same temperature. The cause of deactivation over impregnated catalyst is due to H_2O and/or O_2 in the reaction gas (Tanaka *et al.*, 2003a).

Saito *et al.* (2003) stated that the activity of the Cu/ZnO-based catalysts can be affected by pre-treatments and additives. A $Cu/ZnO/Al_2O_3$ and a $Cu/ZnO/ZrO_2/Al_2O_3$ catalyst were prepared by a CP method. The activity of the $Cu/ZnO/Al_2O_3$ catalyst treated in H_2 at 573 or 723 K decreased with an increase in the calcination temperature. On the other hand, in the case of the $Cu/ZnO/ZrO_2/Al_2O_3$ catalyst, the activity of the catalyst calcined at 773 K and reduced at 573 K was the highest. This finding suggests that the $Cu/ZnO/ZrO_2/Al_2O_3$ catalyst would be less affected by the pre-treatments such as calcination and treatment in H_2 at high temperatures than the $Cu/ZnO/Al_2O_3$ catalyst. Therefore, the $Cu/ZnO/ZrO_2/Al_2O_3$ catalyst should be more practical than the $Cu/ZnO/Al_2O_3$. Also the activity of the $Cu/ZnO/ZrO_2/Al_2O_3$ catalyst calcined at temperatures ranging from 773 to 923 K was higher than those of the catalysts calcined at 673 and 973 K, and also about two times higher than that of the industrial catalyst (Saito and Murata, 2004).

The effect of promoter concentration is another issue in the activity of the catalysts. In the case of Mn-promoted Cu/Al_2O_3 catalyst, the CO conversion increases first with Mn concentration in the catalyst reaches a maximum at 8.55 weight per cent loading and then decreases for higher loadings of Mn. The decrease in CO conversion may be due to the drop in copper surface area at higher copper loadings. The Mn-promoted Cu/Al_2O_3 catalysts are found to be structure sensitive for the LT-WGS reaction (Yeragi *et al.*, 2006). Addition of 0.1 at. per cent of Mg causes a significant increase in the CO conversion as well as in the Cu metal surface area. The formation of Cu^+ species is enhanced by the addition of Mg to the HP-Cu/ZnO catalyst (Shishido *et al.*, 2006b).

Cu-based mixed oxides have different WGS activities when compared to $Cu/ZnO/Al_2O_3$. Among the catalysts studied by Tanaka and coworkers (2003b), $CuAl_2O_4$ showed a relatively high activity in lower temperatures, while $CuMn_2O_4$ exhibited very high CO conversion comparable to the equilibrium conversion over 200^oC. The CO conversions over La_2CuO_4 were not so high, while $CuCr_2O_4$, CuY_2O_5 and $CuFe_2O_4$ were inactive at 200^oC. The order of catalytic activity at 200^oC was M= Mn>Al>La>Cr>Fe>Y, where M is the second component in CuM_2O_4.

The activity of Cu-ZnO catalysts for the WGS reaction was largely influenced by both the kind of support and the reduction temperature. Cu-ZnO catalysts supported on Al_2O_3, MgO and CeO_2 showed high activity, while those on SiO_2-Al_2O_3, SiO_2-MgO and β-zeolite showed less activity in the temperature range 423-523 K (Yahiro *et al.*, 2007). On the other hand, the addition of ceria decreased the amount of available Cu surface area in the study of Koryabkina and coworkers (2003). They applied the fuel reformer conditions for the reaction (7 per cent CO, 8.5 per cent CO_2, 22 per cent H_2O, 37 per cent H_2 and 25 per cent Ar). The findings suggest that ceria is not a promoter.

Copper-based catalysts are generally more active for the shift reaction, but are more unstable to oxidant gases than precious metals. It is, therefore, important to develop highly stable Cu-based catalysts. Ceria supported catalysts are the alternatives to the commercial ones (Shishido *et al.*, 2006a). They are non-pyrophoric and stable, showing little or no deactivation during the experiments and shutdown start-up cycling. The promotion of WGS activity is one of the main roles played by ceria in the automobile three-way catalysts, due to its ability to undergo fast reduction/oxidation cycles depending on the stoichiometry of the exhaust gases. In addition, it stabilizes the active phase in a highly dispersed state and increases the thermal stability of the alumina support (Harrison *et al.*, 1988; Trovarelli, 1996).

Different techniques can be applied to prepare ceria supported catalysts. The activity of the catalysts prepared by deposition-precipitation (DP) is higher than that of the ones prepared by modified deposition- precipitation (MDP). Copper enhances the activity of ceria and Cu/ceria catalysts are more active than the Ag/ceria catalysts which are almost completely inactive because metallic silver adsorbs very weakly CO (Tabakova *et al.*,

2006). Also the nature of the solvent used in the preparation method affects the activity. The impregnated ceria supports prepared from aqueous solutions present higher activities than those prepared from organic solutions (Zerva and Philippopoulos, 2006).

$Cu_xCe_{1-x}O_{2-y}$ catalyst can be prepared by a sol-gel and co-precipitation (CP) method. The $Cu_{0.2}Ce_{0.8}O_{2-y}$ catalyst prepared by CP method showed good activity for the LT-WGS reaction. The $Cu_{0.1}Ce_{0.9}O_{2-y}$ catalyst prepared by sol-gel method was found to be less active, which can be due to lower amount of copper sites, or to different CuO crystallite size and structure (Kusar *et al.*, 2006). These results are also confirmed in the study of Pintar *et al.* (2007). The modification of ceria with Cu^{2+} enhances the ceria reducibility and promotes the creation of surface oxygen vacancies.

Li *et al.* (2000) examined the activity of Cu/CeO_x catalyst which was active for the LT-WGS reaction at much lower temperatures than ceria alone. The catalysts were prepared in nanocrystalline form by the urea gelation co-precipitaiton (UGC) method. Lanthanum dopant (10 at. per cent) was used as a structural stabilizer of ceria. At temperatures below 300^{o}C, five at. per cent $Cu\text{-}Ce(La)O_x$ catalyst indicated similar activity to the activated commercial LTS catalyst. Different copper contents from five to 40 at. per cent showed that there was no appreciable difference in the light-off temperature of the reaction over these ceria-based catalysts. This indicated that only a small amount of copper is adequate to change the WGS activity of ceria. The effect of addition of about 40 per cent hydrogen into the feed gas mixture on the conversion of CO was examined. The results suggested that hydrogen did not significantly suppress the reaction. Above approximately 350^{o}C, there was a decrease in the CO conversion due to the lower equilibrium value at this high concentration of hydrogen.

The LT-WGS reaction was also carried out using different catalysts. A series of carbon nanofiber (CNF) containing Cu-Ce-Zr mixed metal oxide (MMO) catalysts were prepared by homogeneous co-precipitation with urea. The catalytic performance of the CNF-containing samples was compared with that of the corresponding CNF-free Cu-Ce-Zr mixed oxide sample. The CNF-containing samples exhibited a higher activity than the CNF-free catalyst only when based on the metal content. The main advantage of the nanocomposites relates to conserving raw materials for MMO catalysts, since about 13

weight per cent of the MMO could be replaced by CNF without decreasing the overall activity of the catalyst. CNF is also a recycling-friendly additive in MMO materials, since they can be easily removed by oxidation at 400^{o}C (Huber *et al.*, 2007).

The series of Ni-Mo-sulfided catalysts supported on γ-Al_2O_3, TiO_2 and ZrO_2 were tested in the WGS reaction with sulfided feed. The best performance was found for catalysts supported over TiO_2, both Ni-free and containing three weight per cent of Ni. High activity of TiO_2-supported catalysts can be related to better homogeneity in the coordination of Mo species on titania than on alumina or zirconia (Laniecki *et al.*, 2000).

The LT-WGS reaction was also investigated over nickel-molibdenum (Ni-Mo) carbide catalysts at 453 K. In this study, Ni-Mo oxides with various compositions were carburized at different temperatures. The $Ni_{0.25}Mo_{0.75}$ carburized at 873 K exhibited the highest CO conversion rate for all other catalysts. The results indicate that the addition of nickel to the Mo precursor suppressed the catalyst deactivation and enhanced the catalytic activity. The highest active catalyst was an incompletely carburized catalyst (Ni-Mo oxycarbide) containing some remaining oxygen atoms. The increase in the WGS activity was likely due to carbon-deficient sites and the Ni atoms of the Ni-Mo oxycarbides (Nagai *et al.*, 2006). The carburization was also applied to the cobalt-molybdenum (Co_xMo_{1-x}) oxides. The $Co_{0.5}Mo_{0.5}$ carburized at 873 K was found to be the most active among Co-Mo carbide catalysts. Again, the incomplete carburization of the Co-Mo oxide formed the amorphous Co-Mo oxycarbide, leading to a high activity for the LT-WGS reaction (Nagai and Matsuda, 2006).

2.3.2.2. Precious (Noble) Metal Catalysts. Precious metal active components include gold and platinum group metals such as platinum, palladium and ruthenium (Anderson and Boudart, 1982).

Noble metal catalysts usually do not require a lengthy reduction and commissioning process, they are stable to condensing water and air experienced during start/stop operations and can withstand temperature upsets in the process. They also are generally more resistant to poisoning than base metal catalysts and are structurally more stable when washcoated onto monoliths. Their high activity and therefore the ability to build compact

reactors with low pressure drop permit a rapid response to transient conditions, which is another advantage. Precious metals are non-toxic and can be recycled and reused (Ruettinger *et al.*, 2006).

Noble metal/reducible oxide systems have advantages not shown by the traditional catalysts as they can combine high activity and stability (Mendelovici and Steinberg, 1985). Most of the previous work on precious metal LT-WGS catalysts was focused on ceria as the support material for the precious metals (Ruettinger *et al.*, 2006). Ceria is a crucial component, primarily for its role in oxygen storage, the taking up of oxygen under oxidizing conditions and releasing oxygen under reducing conditions. However, the role of ceria as a support for noble metal-based catalyst is not only related to its high oxygen storage capacity but also to the improved dispersion of the noble metal and the promotion of the WGS reaction (Andreeva *et al.*, 2002). Reducibility of surface ceria strongly depends on ceria domain size as well as the degree of interaction with the noble metal. The role of the metal is to catalyze the reduction of surface shell of ceria (Jacobs *et al.*, 2003). Several metal/support associations have been studied. Among those systems Pt/CeO_2 catalyst seems to be the most promising so far, exhibiting good performance (Farias *et al.*, 2007).

The impact of the Pt promoter loading in Pt/CeO_2 catalysts is very important on the catalyst structural-property relationships. Increasing the Pt loading had a significant impact on the catalytic activity. Addition of Pt catalyzes the surface reduction process and reduces the reduction temperature. This indicates that with higher Pt loading, the WGS rate may be higher (Jacobs *et al.*, 2005b).

An acceptable WGS catalyst must be resistant to deactivation under all duty cycles required for the system. However, the deactivation of Pt/CeO_2 WGS catalyst is possible due to start-up/shut-down. Catalyst deactivation can be due to many reasons. Liu *et al.* (2005b) states that the deactivation of the Pt/CeO_2 catalysts is due to the formation of carbonates on the catalyst surface during expected shut-downs in reformate. The carbonates cover the CeO_2 surface, block the Pt metal surface and exert effects on the Pt metal electronic properties. Also, the regeneration of this catalyst can occur by a treatment in air at temperatures greater than 400^oC.

The modification of the Pt/CeO_2 system was investigated in the study of Farias *et al.* (2007). The results indicated that the addition of MgO to Pt/CeO_2 increased the activity and stability of the catalyst irrespective of the preparation method used, either impregnation or CP. The presence of magnesium also improved ceria reduction favoring the creation of OH groups, which are considered to be the active sites for the WGS reaction.

Ceria is not used alone as a catalyst, but it is usually employed in combination with other oxides or in conjunction with active metals and thermally stable supports (Zerva and Philippopoulos, 2006). Recently it is suggested that ZrO_2-CeO_2 composites may be another choice as the support. A ceria-zirconia-rare earth oxide support with 30 per cent CeO_2 content was impregnated with two or three per cent Pt. Start-stop cycles did not lead to significant additional loss of activity, indicating that the (hydroxyl) carbonate build-up observed on Pt on CeO_2 surfaces during this operational mode was suppressed by the addition of ZrO_2 to the support in a mixed oxide (Ruettinger *et al.*, 2006). A series of Pt-promoted ceria-zirconia mixed oxides was prepared, characterized and tested for the LT-WGS reaction. The HP method was used to prepare ceria and zirconia, platinum was added by standard incipient wetness impregnation. The WGS rates were higher for the Zr doped cerium catalysts, promoted with Pt, than either the Pt/ceria or Pt/zirconia undoped catalysts. The catalysts promoted with Zr were found to be less sensitive to irreversible deactivation by co-fed carbon dioxide. However, from a kinetic viewpoint, Pt/ceria, Pt/zirconia and Pt/ceria-zirconia catalysts all decreased in CO conversion with CO_2 addition to the feed. The only benefit with Zr addition to the catalysts appeared when CO_2 was switched off, whereby the catalysts were observed to exhibit a better activity recovery (Ricote *et al.*, 2006).

Researchers have also investigated decreasing of platinum loading in the catalysts due to the high cost of platinum. Radhakrishnan and coworkers (2006) examined the WGS activity of Pt/Re catalysts supported on ceria-zirconia oxides. Nanocrystalline, high surface area ceria-zirconia was prepared using urea homogeneous crystallization co-precipitation. Platinum was deposited on the calcined oxide using a modified ion-exchange method to insure very high metal dispersion. The results indicated that adding about one weight per cent rhenium to a ceria-zirconia supported platinum catalyst was optimal for enhancing

WGS activity over mono-metallic platinum catalysts. Increasing the platinum loading to three weight per cent (without any rhenium addition) provided a similar activity enhancement when compared to the 2:1 Pt/Re sample. Therefore, the optimal platinum to rhenium ratio for these catalysts is approximately 2:1 where the platinum loading is about two weight per cent and this catalyst is selected for further optimization in a fuel processor due to its lower cost potential when commercialized.

$Pt/CeO_2/Al_2O_3$ catalysts are cited as promising catalysts for CO clean-up for on-board applications as they are highly active and non-pyrophoric. A monolith-based design not only gives the required mechanical strength but also leads to better Pt utilization and thus smaller reactor volumes compared to a fixed bed configuration using industrial size catalysts (Quiney *et al.*, 2006).

The nature of oxide supports has a crucial effect on the performance of Pt-based catalysts in the LT-WGS reaction. Supports not only determine the activity of the catalyst, but also influence their stability (deactivation mechanism). Different supports can also be used for the Pt catalysts in LT-WGS reaction. Iida *et al.* (2006) investigated the activities and the characteristics of Pt/TiO_2 (R: rutile) catalysts prepared by a conventional impregnation method. The results state that there is a linear relationship between the catalytic activity and Pt dispersion and that there is little dependency of the catalytic activity on the type of Pt precursors used. The turnover frequency (TOF) for LT-WGS is almost constant regardless of Pt dispersion. This result suggests that LT-WGS reaction on Pt/TiO_2 (R) is structure insensitive.

The effect of morphology of the support on catalytic performance has been investigated over Pt catalysts supported on four commercial titanium dioxide carriers with different structural characteristics (surface area, primary crystallite size of TiO_2). It has been found that conversion of CO at low temperatures ($<300^oC$) is significantly improved when Pt dispersion on TiO_2 samples of low crystallite size. The turnover frequency of CO increases exponentially with decreasing the primary crystallite size of TiO_2, accompanied by a substantial decrease of the apparent activation energy of the reaction. It is concluded that TiO_2-supported noble metals with proper structural and morphological characteristics (high metal dispersion, small TiO_2 crystallite size) may be considered as promising

candidates for the LT-WGS reaction for fuel cell applications (Panagiotopoulou and Kondarides, 2004). Same results were obtained again in the study of Panagiotopoulo *et al.* (2006).The effect of primary particle size of TiO_2 on the reducibility of Pt/TiO_2 catalysts was investigated. It can be concluded that the reaction rate depends strongly on the type of TiO_2 carrier used and increases with increasing surface area of the support or, conversely, with decreasing the primary particle size of TiO_2. The WGS activity of the Pt/TiO_2 catalysts is related to the particle size-dependent reducibility of the titania support. The activity increases with increasing reducibility of TiO_2.

Catalyst stability with time on stream is one key factor that must be taken into account when considering commercial applications of the catalyst. The addition of Re to Pt/TiO_2 improved the catalyst stability in the study of Azzam *et al.* (2007). The catalyst showed almost no deactivation during 20 h time on stream. It is remarkable that Re not only stabilized the Pt/TiO_2 catalyst, but also enhanced activity, that is, the rate of H_2 production. Re addition was also investigated by Iida and Igarashi (2006). The findings indicated that Re addition to Pt catalysts resulted in a decrease in the strength of CO adsorbed on the Pt/TiO_2 (rutile). It was therefore thought that the decreasing strength of CO brought about an increase in the reactivity of the adsorbed CO species due to Re addition.

There are some reports in the literature for LT-WGS reaction over other supported precious metal catalysts. Wang and Gorte (2003) examined the addition of oxide promoters to Pd/ceria catalysts for the LT-WGS reaction. Oxides of Fe, Tb, Gd, Y, Sn, Sm, Eu, Bi, Cr, V, Pb and Mo were added to ceria by wet impregnation. While most of the oxides had a negligible effect on the WGS rates, rates on the Fe-promoted sample were eight times higher than on the unpromoted Pd/ceria at 200^{o}C, while rates on the Mo- and Pb-promoted ceria were significantly lower than on pure Pd/ceria. Hilaire *et al.* (2001) investigated the WGS reaction activities of Pd/ceria, Ni/ceria, Fe/ceria, Co/ceria and Pd/silica catalysts. Pd/ceria exhibited much higher activities than either ceria alone or Pd/silica, demonstrating a cooperative effect between Pd and ceria. Pd/ceria and Ni/ceria showed essentially the same activities and were much more active than either Co/ceria or Fe/ceria.

Ruthenium is another member of platinum-group metals. Basinska and Domka (1999) studied the influence of lanthanum, cerium and samarium used as modifiers of carriers of the Ru/Fe_2O_3 catalysts on their activity in the WGS reaction at 300 or 350°C. The introduction of lanthanides, La^{3+} and Sm^{3+}, led to a much better performance of the catalysts allowing over 90 per cent conversion in WGS reaction. The maximum activity of the catalysts was achieved for the molar ratio of Ru:lanthanide = 1:1.

Ru catalysts supported on CeO_2, La_2O_3, MgO, Nb_2O_5, Ta_2O_5, TiO_2, V_2O_5 and ZrO_2 were investigated for WGS reaction. The CO conversion over Ru/La_2O_3 and Ru/MgO was low below 300°C, while the high conversion above 400°C led to high CH_4 yields over 40 per cent. The CO conversion and CH_4 yield over Ru/Nb_2O_5 increased from 300°C to the level over 90 and 40 per cent at 425°C, respectively. The above-mentioned Ru catalysts were active only for the methanation. On the other hand, Ru catalysts supported on TiO_2, V_2O_3 and ZrO_2 had some activity for the shift reaction while producing little amounts of methane in the limited reaction temperature region. The shift reaction proceeded at 150 and 200°C over Ru/ZrO_2, though the CO conversion was low. The production of methane increased with reaction temperatures above 200°C. The Ru/V_2O_3 catalyst reduced at 400°C had the highest activity for the shift reaction without producing methane. The Ru/La_2O_3 catalyst did not adsorb CO (Utaka *et al.*, 2003).

Recent studies of the LT-WGS reaction have shown also that supported gold catalysts are active catalysts for this reaction (Leppelt *et al.*, 2006). The prerequisite for the synthesis of a highly active gold supported catalyst is not only to obtain a high dispersion of gold particles but also to choose an appropriate support for the reactions. The activity and especially the stability of the gold catalysts depend on both the state and the structure of the support and the specific interaction between gold and the support (Andreeva *et al.*, 2002). Therefore, the WGS reaction activities of supported gold catalysts are mainly governed by three factors: (i) nature of the support used, (ii) gold particle size, (iii) method of preparation, which depended again on pH, preparation temperature, type of active precursor, precipitating agent.

The role of ceria as a support and the effects of the gold content for Au/CeO_2 catalysts were investigated. The sample with the highest gold loading (five weight per cent

Au/CeO_2) exhibited the highest CO conversion. On the other hand, the three weight per cent Au/CeO_2 sample exhibited the highest stability. Also the size of the gold particles was not only preserved after operation, but even tended to decrease. This effect could be connected with the strong interaction between the gold particles and the ceria surface (Andreeva *et al.*, 2002).

The synthesis of nanosized gold catalysts is highly sensitive towards the preparation technique which determines a great difference in the size of gold particles and in their interaction with the support. Conventional impregnation method is not suitable to prepare gold catalysts. Gold/ceria catalysts were prepared by two different methods: deposition-precipitation (DP) and modified deposition-precipitation (MDP). The CO conversion over Au/ceria catalyst prepared by DP is significantly higher than over prepared by MDP up to 200^{o}C. The DP method allowed preparation of catalysts with narrower particle size distribution where Au was mainly localized on the surface of the support. The higher amount of gold exposed on the surface of catalyst prepared by DP as a consequence of higher gold dispersion (Tabakova *et al.*, 2004).

Fu *et al.* (2003) studied nanostructured Au/ceria prepared by DP, CP and urea gelation co-precipitation (UGC) methods. The gold loading was varied between one and 8.3 at. per cent while lanthanum used as a dopant in ceria four or 10 at. per cent. A uniform distribution of gold on ceria was found for the DP sample, while the CP sample contained relatively large gold particles with a lower dispersion. Also the addition of La inhibited the crystal growth of ceria made by either the CP or the UGC methods.

Kim and Thompson (2005) examined the deactivation for a series of CeO_2-supported gold catalysts for the LT-WGS reaction. The catalysts designed to have loadings of five weight per cent Au were prepared by the DP method. The catalytic properties were measured at temperatures ranging from 200 to 240^{o}C. The most active catalyst was the Au/CeO_2 calcined at 400^{o}C; however, its activity decreased by more than 50 per cent during the first 12 h on-stream. The results indicated that deactivation was due to the formation of carbonates and/or formates on the catalyst surface. Initial activities for the Au/CeO_2 catalysts could be fully recovered by calcination of the deactivated catalysts in flowing air at elevated temperatures.

Most of the earlier studies were performed in idealized reaction gas mixtures, mainly in dilute water-gas (CO, H_2O, inert). The LT-WGS reaction on Au/CeO_2 catalysts in idealized reaction atmosphere (1 kPa CO, 2 kPa H_2O) and the effect of catalyst loading were investigated. Comparing the activity of one, three, five weight per cent Au/CeO_2 catalyst in conversion measurements, it was found that the best performance was exhibited by three weight per cent catalyst, closely followed by the five weight per cent Au catalyst (Leppelt *et al.*, 2006). The reaction in realistic reformate has been investigated only in a limited number of studies (Kim and Thompson, 2005; Fu *et al.*, 2005; Sakurai *et al.*, 2005). Denkwitz *et al.* (2007) reported on the effect of CO_2 and H_2 and of more realistic CO and H_2O concentrations on the activity and, in particular, the deactivation of Au/CeO_2 catalysts. Kinetic measurements revealed that H_2 significantly reduced the initial reaction rate but had little effect on deactivation. In contrast, the effect of CO_2 on the reaction rate was small but resulted in a much more pronounced deactivation. This latter effect increased with increasing CO_2 content and was mainly responsible for the enhanced deactivation in realistic reformate.

Ceria supports for gold catalysts in LT-WGS reaction were also applied in combination with alumina. Andreeva *et al.* (2006) studied the gold catalysts supported on ceria and ceria-alumina with different ratios. The catalysts were prepared by CP method and pretreated in H_2/Ar mixture. The catalysts on mixed ceria-alumina supports exhibited lower activity comparing to gold-ceria sample. The pretreatment in H_2/Ar mixture did not influence the activity of gold-ceria catalyst while the WGS activity of the samples on ceria-alumina decreased. Also, the presence of alumina led to an increase of the average size of gold particles in the fresh samples and to decrease of the ceria particles size. During the catalytic operation, both gold and ceria dispersion practically did not change in the presence of alumina; this was an indication of the improved stability of the catalysts supported on ceria-alumina.

Different supports can be tested for gold catalysts in LT-WGS reaction. In the study of Andreeva *et al.* (1998) it has been shown that $Au/\alpha\text{-}Fe_2O_3$ catalysts manifest high catalytic activity in the LT-WGS reaction. $Au/\alpha\text{-}Fe_2O_3$ catalysts are commonly prepared by CP; but, in this study it was also prepared by a MDP method. $Au/\alpha\text{-}Fe_2O_3$ catalyst prepared by MDP manifested a higher conversion degree in the investigated range than the Au/α-

Fe_2O_3 sample prepared by CP. This sample also demonstrated higher stability than the co-precipitated sample. MDP method led to a much more uniform gold particle size distribution on α-Fe_2O_3.

The LT-WGS activity and stability of Au/Fe_2O_3 is improved upon addition of the metal oxides. The activity and stability of the catalyst is increased significantly by addition of ZrO_2 and to a lesser extent MgO, CaO, NiO, La_2O_3, Cr_2O_3, CuO. In contrast, Bi, Ti and Mn oxides seriously decrease the catalytic activity while additions of Zn, Al, Ba, Co, Ce and Mo oxides do not influence evidently the catalytic activity and its stability. The improvement of catalytic stability may be attributed to the comparative stabilization of high dispersion of gold particles and uneasily sintering of Fe_3O_4 crystallites during the catalytic operation (Hua *et al.*, 2005).

The LT-WGS reaction has been carried out over Au-Ru supported on α-Fe_2O_3 catalyst by Venugopal *et al.* (2003). The activity of the bimetallic Au-Ru/iron oxide has been compared with Au/iron oxide and Ru/iron oxide catalysts. The Au-Ru/iron oxide and Ru/iron oxide samples show almost identical conversions, both catalysts being more active than Au/iron oxide, by at least a factor four for temperatures of 200^{o}C and above. Also it is noted that the decrease in specific surface area is considerably less in the case of the Au-Ru/iron oxide sample compared with the situation found for Au/iron oxide and Ru/iron oxide.

It has been established that the gold catalysts on well crystallized supports, Au/Fe_2O_3 and Au/ZrO_2, display higher catalytic activity in the WGS reaction in comparison with the samples on amorphous and not well crystallized supports-Au/ZnO, Au/ZrO_2, Au/Fe_2O_3-ZnO and Au/Fe_2O_3-ZrO_2. The catalytic activity of the samples on the mixed oxide supports is lower in the low temperature range and the sample Au/Fe_2O_3-ZnO displays a higher conversion degree compared to Au/Fe_2O_3-ZrO_2 (Tabakova *et al.*, 2000).

It is anticipated that the use of a high surface area mesoporous oxide support for noble metals or transition metals has some beneficial effect on the catalytic performance (Velu *et al.*, 2003). The mesoporous support would give rise to well dispersed and stable metal particles on the surface upon calcination and reduction and as a consequence would

show an improved catalytic performance. Therefore, the WGS reaction was carried out over gold catalysts supported on mesoporous titania. The mesoporous titania with high surface area and uniform pore size distribution was synthesized by surfactant templating method. Different gold content (one-five weight per cent), was loaded on mesoporous titania by DP method which can provide nanometer size gold particles. High and stable WGS activity of this catalyst could be related to the high stability of the gold dispersion. Also higher activity was obtained for the sample with lower average size of the gold particles and lower gold content (Idakiev *et al.*, 2004). Besides Au-mesoporous TiO_2, the catalytic behaviour of Au-mesoporous ZrO_2 was also studied in the temperature range 140-300^oC. The sample with higher gold content manifested high CO conversion even at rather low H_2O/CO ratios. These Au-mesoporous zirconia catalysts had even higher WGS activity than the reported Au-mesoporous titania (Idakiev *et al.*, 2006).

Comparative studies for LT-WGS reaction was carried out by researchers. The activity of the Pt/CeO_2 prepared by sol gel, Au/CeO_2 prepared by CP and Au/Fe_2O_3 prepared by either CP or DP was tested in the comparison of four per cent CO, 2.6-20 per cent H_2O and helium in the range of 120-360^oC. It was found that CO and H_2O concentrations have significant effects on the catalytic activity. It was observed that water had a positive effect on the Pt/CeO_2 catalysts and a moderate positive effect on the Au/CeO_2 and Au/Fe_2O_3 catalysts. The catalytic activity and stability tests showed that activity of gold-containing catalysts was decreasing during the catalytic tests. Pt/CeO_2 catalyst showed good stability compared to the other two catalysts. Pt/CeO_2 catalysts seemed to be appropriate for WGS reaction at moderate reaction conditions and high H_2O/CO in comparison with the Au catalysts in the presence and absence of H_2. The one per cent Pt/CeO_2 was substantially more active than other catalysts in the presence of 20 per cent H_2O (Luengnaruemitchai *et al.*, 2003).

2.3.3. Low-temperature Water-Gas Shift Reaction Mechanism and Kinetics

Although numerous mechanistic and kinetics studies have been carried out in recent years, disagreement remains about the nature of the reaction intermediates and the active sites of metal supported on redox oxides. Two reaction mechanisms for LT-WGS are mainly proposed in the literature: the “adsorptive or associative mechanism” and the

"redox mechanism". In the adsorptive or associative mechanism, CO and H_2O are proposed to adsorb on the catalyst surface and form a surface intermediate, which subsequently decomposes as H_2 and CO_2 (Tibiletti *et al.*, 2006).

(i) $CO + * \rightarrow CO_{ad}$ (2.27)

(ii) $H_2O + 2* \rightarrow H_{ad} + OH_{ad}$ (2.28)

(iii) $OH_{ad} + CO_{ad} \rightarrow HCOO_{ad} + *$ (2.29)

(iv) $HCOO_{ad} + * \rightarrow CO_{2,ad} + H_{ad}$ (2.30)

(v) $2H_{ad} \rightarrow H_2 + 2*$ (2.31)

where "*" is a general adsorption site (Gorte and Zhao, 2005). Many research groups have tried to identify the nature of the main intermediate species (Tibiletti *et al.*, 2006; Choi and Stenger, 2003). Formate species have been proposed for the forward-WGS reaction (Shido and Iwasawa, 1993; Jacobs *et al.*, 2004) and carbonates for both the forward and reverse-WGS reaction (Koeppel *et al.*, 1991). In work published by Ricote *et al.* (2006), it has been proposed that one of the metal's main roles would be to favor the formation of reactive surface hydroxyl groups (type II) on the oxide support, which would lead to increased formation of formate species. In the redox mechanism, water adsorbs and dissociates on reduced sites of catalyst surface to produce hydrogen while oxidizing a site. In parallel, CO is oxidized to CO_2 on these oxidized sites.

(i) $H_2O + Red \rightarrow H_2 + Ox$ (2.32)

(ii) $CO + Ox \rightarrow CO_2 + Red$ (2.33)

where "Red" represents a reduced site and "Ox" an oxidized site (Choi and Stenger, 2003).

Ceria has been well characterized and it is well established that reduced centers at the surface are involved in the catalysis. Although some researchers favor a redox mechanism to explain the catalysis of LT-WGS and others favor a formate-based mechanism, at this time there is a general consensus that reduced centers are involved in the catalysis of both schemes, which are delineated as follows where Ce=Ce^{4+} and **Ce**=Ce^{3+} (Jacobs *et al.*, 2005a):

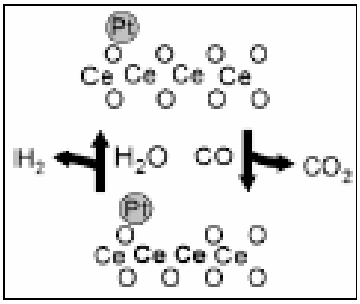

Figure 2.1. Ceria-mediated redox mechanism (Jacobs *et al.*, 2005a)

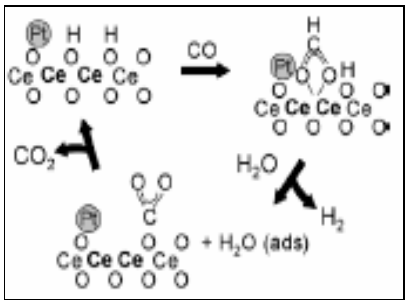

Figure 2.2. Formate mechanism (Jacobs *et al.*, 2005a)

The redox mechanism proposes that the oxidation state of Ce changes between Ce^{4+} and Ce^{3+} during the course of the mechanism, with CO reducing ceria to generate CO_2 and H_2O reoxidizing ceria to liberate H_2. But there is considerable evidence suggesting that bridging OH groups on the surface react with CO to generate surface formates, which decompose in the presence of H_2O to liberate H_2 and produce unidentate carbonate, which decomposes to CO_2. In the surface formate mechanism the rate-determining step has been proposed to be the decomposition of surface formate. Decomposition of formate in the formate mechanism promoted by H_2O; this is why H_2O was included in the transition state of the formate decomposition step of an early formate mechanism of Shido and Iwasawa (1993). The catalytically active sites were found to be type II bridging OH groups on partially reduced ceria.

The formation of bridging OH groups can follow one of two routes on M/ceria (Jacobs *et al.*, 2006).

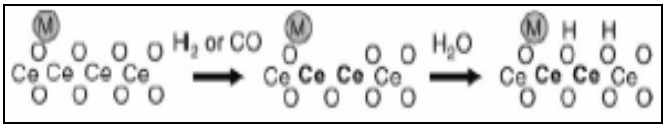

Figure 2.3. Formation of bridging OH groups, Route 1 (Jacobs *et al.*, 2006)

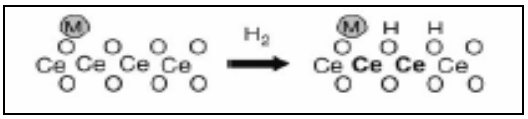

Figure 2.4. Formation of bridging OH groups, Route 2 (Jacobs *et al.*, 2006)

During activation, a reducing gas can remove oxygen at the surface, accompanied by a change in the oxidation state of the Ce involved from Ce^{4+} to Ce^{3+}. H_2O then dissociates on the surface to yield the bridging OH groups, but the oxidation state of the Ce involved remains Ce^{3+}. In the second case, H_2 dissociation on M and spillover to ceria can directly yield the bridging OH groups, again accompanied by a change in the oxidation state of the Ce involved from Ce^{4+} to Ce^{3+} (Jacobs *et al.*, 2005a; Jacobs *et al.*, 2006).

Jacobs *et al.* (2006) studied the LT-WGS reaction and they found that a surface formate (associative) mechanism best described the Pt/ceria catalysts. Also, the Pt catalysts were found to be far more active than the Au catalysts. The influence of Pt loading on the degree of ceria partial reduction in the low temperature range was investigated. It was found that the addition of Pt catalyzes the surface reduction process and reduces the peak reduction temperature (Jacobs *et al.*, 2005b).

Hilaire *et al.* (2001) have presented arguments against the surface formate mechanism and used these arguments to serve as the basis to support a ceria-mediated redox process as Bunluesin *et al.* (1998).

(i) $CO + \blacksquare \rightarrow CO_{ad}$ (2.34)

(ii) $H_2O + Ce_2O_3 \rightarrow 2CeO_2 + H_2$ (2.35)

(iii) $CO_{ad} + 2CeO_2 \rightarrow CO_2 + Ce_2O_3 + \blacksquare$ (2.36)

where "■" represents the adsorption sites on the metal (Bunluesin *et al.*, 1998; Hilaire *et al.*, 2001). They suggested this mechanism for Pd/ceria, Co/ceria, Ni/ceria, Fe/ceria. They have argued that surface formates do not form, as was claimed by Shido and Iwasawa (1993). Upon closer examination of reported spectra, it becomes clear that the range of wavenumbers and the bands examined in their Fourier transform infrared (FTIR) spectra are not complete. They make the claim that, based on spectra in the 1000-1700 cm^{-1} range, only carbonates form. However, the bands which appear in this region are for OCO asymmetric and symmetric stretching vibrations. Therefore, it is difficult to distinguish whether bands in this region correspond to carbonates or formates, because both species contain OCO vibrations (Jacobs *et al.*, 2004).

From the proposed mechanisms, a variety of rate expressions can be derived (Choi and Stenger, 2003). From the associative mechanism, Langmuir-Hinshelwood type rate expression can be derived. When the surface reaction is assumed rate controlling:

$$r_{CO} = k\frac{P_{H_2O}P_{CO} - P_{H_2}P_{CO_2}/K_p}{(1+K_1P_{CO}+K_2P_{H_2O}+K_3P_{CO_2}+K_4P_{H_2})^2} \tag{2.37}$$

The above rate expression has been tested using plant and laboratory data by several authors (Amadeo and Laborde, 1995), who report that only the Langmuir-Hinshelwood model can accommodate all of the experimental data. Alternatively, single path reaction mechanism applied to the associative mechanism results in the following expressions (Fiolitakis and Hofmann, 1983)

$$r_{CO} = k\frac{P_{H_2O}P_{CO} - P_{H_2}P_{CO_2}/K_p}{1+K_1P_{H_2O}+K_3P_{CO_2}} \tag{2.38}$$

For the redox mechanism, the following rate expression was derived and its validity was confirmed using Cu-Zn-Cr catalysts.

$$r_{CO} = k\frac{P_{H_2O}P_{CO} - P_{H_2}P_{CO_2}/K_p}{AP_{H_2O}+P_{CO}} \tag{2.39}$$

Using a CuO/ZnO catalyst, another rate expression can be derived from the redox mechanism when a single path reaction model is assumed (Fiolitakis and Hofmann, 1983).

$$r_{CO} = \frac{k_1 k_2 (P_{H_2O} P_{CO} - P_{H_2} P_{CO_2} / K_p)}{k_1 P_{H_2O} + k_2 P_{CO} + (k_{1-} + k_{2-}) P_{CO_2}} \tag{2.40}$$

In contrast to those rate expressions from detailed reactions, mechanisms and rate-determining steps, there are simple empirical rate expressions which do not consider any mechanism (Choi and Stenger, 2003).

$$r_{CO} = k(P_{CO} P_{H_2O} - \frac{P_{CO_2} P_{H_2}}{K_p}) = k P_{CO} P_{H_2O} (1 - \beta) \tag{2.41}$$

$$\beta = \frac{P_{CO_2} P_{H_2}}{P_{CO} P_{H_2O} K_{eq}} \tag{2.42}$$

Choi and Stenger (2003) offered an empirical power-law rate expression derived from numerical fitting for water-gas shift reaction between 120-250^{o}C running over Cu/ZnO/Al_2O_3 catalyst:

$$r_{WGS} = 2.96 \times 10^5 \exp\left(-\frac{47{,}400}{RT}\right)\left(P_{CO} P_{H_2O} - \frac{P_{CO_2} P_{H_2}}{K_{eq,WGS}}\right) \tag{2.43}$$

In addition, a comparison of activation energies of frequency factors with other empirical power-law rate expressions derived from different catalysts are given in Table 2.1 (Choi and Stenger, 2003).

$$r_{WGS} = k_{o,WGS} \exp(-E_{WGS} / RT) P_{CO}^m P_{H_2O}^n (1 - \beta) \tag{2.44}$$

Table 2.1. Parameter comparison for empirical expressions (Choi and Stenger, 2003)

Catalyst	m	n	$\ln k_o$	E_a (kJ.mol^{-1})
$Cu/ZnO/Al_2O_3$	1	1	12.6	47.4
$Cu/ZnO/Al_2O_3$	0	1	-	41.8
Cu/Al_2O_3	1	1.9	-	69.3
Cu/MnO_2	1	1	-	55
ICI-$Cu/ZnO/Al_2O_3$	1	1	15.2	52.8

Other research groups have reported that the WGS reaction is not a simple order reaction, especially at higher steam/CO ratios and have tried to find proper exponent parameters in a power-law type rate equation (Keiski *et al.*, 1993):

$$r_{CO} = kP_{CO}^{n} P_{H_2O}^{m} (1-\beta) \tag{2.45}$$

A power-law rate expression is very useful for the design of reactors. Koryabkina *et al.* (2003) used the same method and reaction steps as described in Ovesen *et al.* (1996). Their mechanism can be represented as (where * is a free site):

(i) $H_2O + * \leftrightarrow H_2O*$ (2.46)

(ii) $H_2O* + * \leftrightarrow OH* + H*$ (2.47)

(iii) $2OH* \leftrightarrow H_2O* + O*$ (2.48)

(iv) $OH* + * \leftrightarrow O* + H*$ (2.49)

(v) $2H* \leftrightarrow H_2 + 2*$ (2.50)

(vi) $CO + * \leftrightarrow CO*$ (2.51)

(vii) $CO* + O* \leftrightarrow CO_2* + *$ (2.52)

(viii) $CO_2* \leftrightarrow CO_2 + *$ (2.53)

It was assumed that: 1) steps (i), (iii), (v), (vi) and (viii) are in equilibrium, 2) the remaining steps (ii), (iv) and (vii) may not be in equilibrium and could be rate-determining, 3) the catalyst surface is composed of mostly Cu (111) planes, which implies that the equilibrium constants and rate constants can be directly taken or calculated from published

literature data on Cu (111) single crystal studies. The kinetic modeling supports the surface redox mechanism with the reduction of surface oxygen by adsorbed CO as the rate-determining step (Koryabkina *et al.*, 2003).

3. EXPERIMENTAL WORK

3.1. Materials

3.1.1. Chemicals

All the chemicals used in catalyst preparation are listed in Table 3.1.

Table 3.1. Chemicals used in catalyst preparation

Chemicals	Formula	Grade	Source	Molecular Weight ($g.mol^{-1}$)
Tetraammineplatinum (II) nitrate	$Pt(NH_3)_4(NO_3)_2$	Research	Aldrich	387.21
Cerium (III) nitrate hexahydrate	$Ce(NO_3)_3.6H_2O$	Extra pure	Merck	434.23
Aluminum Oxide	γ-Al_2O_3	Extra pure	Zeochm EU	101.96

3.1.2. Gases and Liquids

The gases H_2, Ar and CO used in this study were supplied by Birleşik Oksijen Sanayi (BOS) and He was obtained from HABAŞ Company, Istanbul, Turkey. The applications and specifications of the liquids and gases used in this study are listed in the Tables 3.2 and 3.3.

Table 3.2. Applications and specifications of the liquids used

Liquid	Application	Specification
Water	Reactant, Aqueous solutions	Distilled

Table 3.3. Applications and specifications of the gases used

Gas	Application	Specification
Carbon monoxide	Reactant, GC calibration	99.5%
Helium	Reactant (inert), GC calibration	99.999%
Hydrogen	Reducing agent, GC calibration	99.99%
Argon	GC carrier	99.999%

3.2. Experimental Systems

The experimental systems used in this work can be classified mainly into three groups:

1) Catalyst Preparation System: Catalysts are prepared by sequential impregnation method in this system.

2) Microreactor Flow System: This system was constructed and includes mass flow controllers for inlet gases, a liquid pump for water feed, temperature-controlled heated connecting lines and a fixed bed flow reactor in a vertical furnace whose temperature is controlled by a programmable temperature controller. This system is used for catalytic activity tests.

3) Product Analysis System: In this system, the composition of the reactant and product gases is analyzed by using a gas chromatograph.

3.2.1. Catalyst Preparation System

Three groups of Pt-CeO_x/γ-Al_2O_3 catalysts including same Pt content and different CeO_x contents were prepared by sequential impregnation method. The system used for catalyst preparation includes a Retsch UR1 ultrasonic mixer which provides uniform mixing and contact of the solution with the support, a vacuum pump, a Masterflex computerized-drive peristaltic pump which is used for addition of the solution that will be impregnated, a vacuum flask, a beaker and silicone tubing (Figure 3.1).

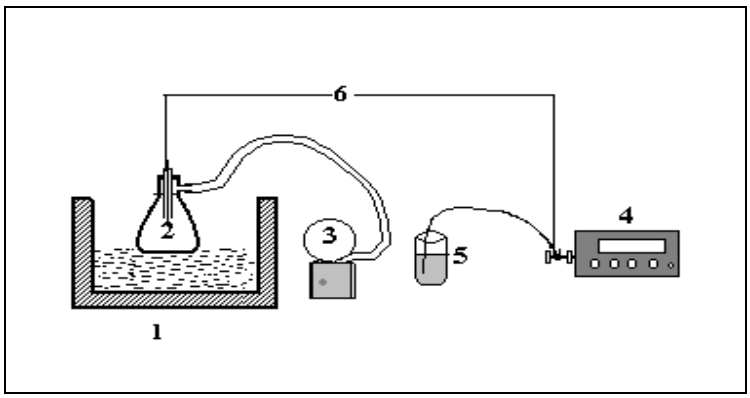

Figure 3.1. The impregnation system: 1.Ultrasonic mixer 2.Vacuum flask 3. Vacuum pump 4.Peristaltic pump 5.Beaker 6.Silicone tubing (Akın, 1996)

3.2.2. Microreactor Flow System

The microreactor flow system used for low-temperature water-gas shift reaction was designed and constructed in the laboratory. This system includes three main sections as shown in Figure 3.2. Details and the necessary equipment for the system are presented in Section 4.

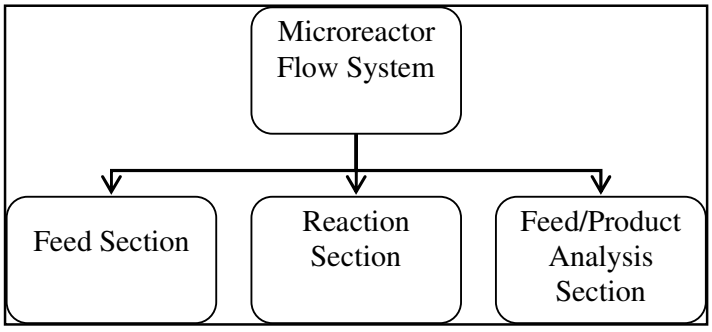

Figure 3.2. Block diagram of the microreactor flow system

3.2.3. Product Analysis System

The reactant and product gas streams were analyzed using an HP-Agilent 6890N Network temperature-controlled programmable gas chromatograph equipped with a thermal conductivity detector (TCD). A Molecular Sieve 5A packed column was used for

detecting the components of the feed and product gases after the reaction and was operated under argon as carrier gas.

The packed column used in this study was prepared in the laboratory. A 1/8" OD x 2 m long stainless steel tube was used as column tubing material. The inside of column tubing was washed with suitable cleansing liquids and then dried by allowing helium to flow through it. One end of the column was plugged with glass wool and the column was packed with Molecular Sieve 5A by vibrating the column to provide uniform packing. After packing, the inlet was also plugged with glass wool and column was coiled.

Before operation, the column was conditioned at 300^{o}C for 12 hours with a column flow of 30 ml.min^{-1} argon. Analysis conditions for the experiments are given in Table 3.4.

Table 3.4. Reactant and product gas analysis conditions

Column Type	Packed Column
Detector Type	Thermal Conductivity
Column Oven Temperature	40^{o}C
Injector Temperature	40^{o}C
TCD Temperature	150^{o}C
Carrier Gas	Argon
Carrier Gas Flow Rate	40 ml.min^{-1}
Column Packing Material	Molecular Sieve 5A, 60-80 mesh
Column Tubing Material	Stainless Steel
Column ID & Length	1/8" OD x 2 m
Sample Loop	1 ml

3.3. Catalyst Preparation

The Pt-CeO_x/γ-Al_2O_3 catalysts used in the experiments were prepared in three groups:

(1) 1.4 wt. per cent Pt-10 wt. per cent CeO_x/γ-Al_2O_3
(2) 1.4 wt. per cent Pt-5 wt. per cent CeO_x/γ-Al_2O_3
(3) 1.4 wt. per cent Pt-1.25 wt. per cent CeO_x/γ-Al_2O_3

Catalysts were prepared by the sequential impregnation method using the system in Figure 3.1. The impregnation method used in this study consists of four steps. These are:

(i) Evacuating the support
(ii) Contacting the support with the precursor solution
(iii) Drying
(iv) Calcination

Commercial γ-alumina support was crushed and sieved into 45-60 mesh size (344-255 μm). It was dried in a furnace at 105^{o}C for 1 hour and then calcined in a muffle furnace at 450^{o}C for 5 hours. For the preparation of catalysts by incipient wetness impregnation method, a definite amount of alumina support was put in a vacuum flask and was kept under vacuum in the first step. The vacuum pump was also kept on during the addition of the precursor solution since the trapped air in the pores of the support could prevent complete penetration of the solution. This treatment provides more uniform distribution of the active component by removing the trapped air. The support material in the vacuum flask was mixed under vacuum with an ultrasonic mixer for 30 minutes before impregnation.

The calculated amount of cerium nitrate salt was dissolved in 1.21 ml of distilled water per gram of alumina support. Aqueous cerium nitrate solution was fed to the vacuum flask at a flow rate of 0.5 ml.min^{-1} via a silicone tubing using a Masterflex computerized-drive peristaltic pump. The slurry was mixed ultrasonically during impregnation to maintain uniform distribution of the cerium nitrate solution. After all the cerium nitrate

solution was fed, the mixing was continued for an additional 90 minutes. The resulting slurry was dried at 115°C overnight (16 hours) and then was calcined at 400°C for 2 hours to obtain $CeO_x/\gamma\text{-}Al_2O_3$.

The calculated amount of Pt precursor salt was dissolved in distilled water and the aqueous solution of Pt was added to the dried, calcined and ceria impregnated alumina catalyst with the same procedure described above. After impregnation, the resulting slurry of $Pt\text{-}CeO_x/\gamma\text{-}Al_2O_3$ catalyst was dried at 115°C overnight (16 hours) and calcined at 400°C for 2 hours to obtain $Pt\text{-}CeO_x/\gamma\text{-}Al_2O_3$.

3.4. Catalytic Activity Experiments

3.4.1. Preliminary Work

3.4.1.1. Gas Chromatograph Calibration. Before starting the experiments, gas chromatograph was calibrated by injecting known amounts of the species separately to the chromatographic column under the conditions given in Table 3.4 and by reading the corresponding retention time and the area under the peak calculated by the integrator software. Using this procedure, peak area versus volume per cent graphs were constructed for each gas and the corresponding calibration curves were determined by linear regression. The calibration curves are presented in Appendix A.

3.4.2. Reaction Tests

All $Pt\text{-}CeO_x/\gamma\text{-}Al_2O_3$ catalysts were reduced in H_2 at 350°C before the reaction and kept under a stream of He until the reaction test was performed. The temperature program used for the reductive pretreatment can be seen in Table 3.5.

Table 3.5. Reduction program for Pt-CeO_x/γ-Al_2O_3 catalysts

Segments	Starting and End Temperatures	Segment Gas
First Segment	Heating from 25°C to 350°C with a heating rate 5°C.min^{-1}	He with flow rate of 50 ml.min^{-1}
Second Segment (Reduction)	Keeping constant at 350°C for 2 or 3h	H_2 with flow rate of 50 ml.min^{-1}
Third Segment	Flushing at 350°C for 1h to clean the catalyst surface	He with flow rate of 50 ml.min^{-1}
Fourth Segment	Cooling down to reaction temperature	He with flow rate of 25 ml.min^{-1}

After reduction, the temperature of the reactor was decreased down to reaction temperature (250, 275, 300, 350°C) under inert helium flow and helium was trapped within the reactor until the reaction gases were sent to the reactor. Stainless steel tubular down-flow microreactor was used for determining the catalytic activities of the Pt-CeO_x/γ-Al_2O_3 catalysts. All experiments were performed at atmospheric pressure. The catalytic activity tests for low-temperature water-gas shift were conducted with the feed mixture of 5 per cent CO, 5 per cent H_2O and He as balance for all catalysts. 5 per cent CO, 10 per cent H_2O in He and 5 per cent CO, 15 per cent H_2O in He feed mixture was applied only to 1.4wt.%Pt-1.25wt.%CeO_x/γ-Al_2O_3 catalyst to see the effect of H_2O/CO ratio on CO conversion. Catalyst weight was 250 mg in all experiments.

The total flow rate, reduction time, reaction temperatures, catalysts and H_2O/CO ratio were changed in order to see the effects of different parameters on the catalyst activity. The reaction conditions for three catalysts are summarized in Table 3.6, and the list of the experiments is given in Table 3.7.

Table 3.6. Reaction conditions for catalytic activity tests

Parameter	Value
Catalyst Particle Size (mesh size)	45-60 (344-255µm)
Catalyst Amount (mg)	250
Reduction Temperature (^oC)	350
Reaction Temperature (^oC)	250, 275, 300, 350
Reaction Total Flow Rate ($ml.min^{-1}$)	100, 150, 200
W/F_{CO} Ratio ($mg.min.\mu mol^{-1}$)	1.22, 0.814, 0.61

Table 3.7. The list of experiments performed on Pt-CeO_x/γ-Al_2O_3 catalysts

Cat. No	Metal Content		Reaction Temperature (^oC)	Reduction Time (h)	Total Flow Rate (ml/min)	Feed Gas Composition in He as balance	
	Pt (wt.%)	CeO_x (wt.%)				CO (vol.%)	H_2O (vol.%)
1	1.4	10	350	3	200	5	5
1	1.4	10	300	2	100	5	5
1	1.4	10	300	2	150	5	5
1	1.4	10	300	2	200	5	5
1	1.4	10	300	3	200	5	5
1	1.4	10	275	3	200	5	5
1	1.4	10	250	3	200	5	5
2	1.4	5	350	3	200	5	5
2	1.4	5	300	3	200	5	5
2	1.4	5	275	3	200	5	5
2	1.4	5	250	3	200	5	5
3	1.4	1.25	350	3	200	5	5
3	1.4	1.25	300	3	200	5	5
3	1.4	1.25	275	3	200	5	5
3	1.4	1.25	250	3	200	5	5
3	1.4	1.25	250	3	200	5	10
3	1.4	1.25	250	3	200	5	15

4. RESULTS AND DISCUSSION

4.1. Design and Construction of the System

The microreactor flow system was designed and constructed in the laboratory with all necessary tubing and fitting materials and auxiliary units. The details of the system designed for conducting low-temperature water-gas shift experiments are presented in Figures 4.1 and 4.2.

The system consisted of three parts:

(i) Feed section
(ii) Reaction section
(iii) Feed/Product analysis section

4.1.1. Feed Section

The feed section was composed of mass flow controllers, 1/4", 1/8" and 1/16" OD stainless steel and brass tubes and fittings for feeding the reactants to the system. In this section, the research grades of pure CO, He, H_2 gases from pressurized cylinders were passed through brass tubes and fittings. The flow rates of the gases were controlled by Brooks 5850E mass flow controllers. The set point values of the flow controllers were adjusted by four-channel Brooks 0154 control panel. Inlet pressure to the flow controllers was 30 psi for all reaction gases, but flow rate ranges of the flow controllers were different. These ranges of the mass flow controllers were selected to provide the desired gas flow rates. The specifications of the mass flow controllers used are given in Table 4.1. The mass flow controllers were calibrated *in situ* and their calibration curves are presented in Appendix B. At the inlet and the outlet of the mass flow controllers, 1/4" stainless steel tubes were used until the primary mixing zone. On-off valves were placed after the mass flow controllers. In order to provide homogeneous mixing, the reactant gases were passed through the primary mixing region before the water feed was introduced. This primary mixing region was constructed using 1/8" stainless steel tubes. The reactant gases were

passed through the heated stainless steel tubing in order to get the sufficient energy to vaporize the water. A 4 m-long heating tape was used to heat the lines and a 16-gauge wire K-type sheathed thermocouple was placed along the heated lines and connected to a temperature controller. The heating tape was covered with ceramic wool insulation to prevent heat losses. The temperature was controlled by Dixel single stage digital controller XT110C. Water was fed to the reaction system at constant flow rates using an Agilent 1200 Isocratic HPLC pump. Distilled water was used for all experiments and it was added after all reaction gases were mixed. Water was allowed to flow through the 1/16" tube and then let into the heated tubes through which the gas mixture passed. The gas mixture and steam were mixed in a secondary mixing region. This secondary mixing region was made using 1/16" stainless steel tube, after which the diameter of connecting lines was gradually increased to 1/8" and 1/4". Gas flow could be diverted using a three way valve. The flow could be sent to vent line in order to ensure the mixing of the steam and the reactant gases to get a steady flow before the reaction or it could be sent to another three way valve. This second valve was used to send the flow to the bypass line, so that feed composition could be analyzed in the gas chromatograph or to the reaction section. An on-off valve was placed at the end of the bypass line. This valve prevented the product gases to fill the bypass line when it was closed.

Table 4.1. Specifications of the mass flow controllers

Gas Type	CO	He	H_2	CO_2
Flow Rate Range ($ml.min^{-1}$)	0-20	0-200	0-100	0-50
Upstream Pressure (psi)	30	30	30	30
Maximum Working Pressure (bar)	100	100	100	100
Ambient Temperature Limits (^oC)	5 to 65	5 to 65	5 to 65	5 to 65

4.1.2. Reaction Section

The reaction section was connected by 1/4" stainless steel tubes and consisted of a 2.6 cm ID x 46.5 cm tube furnace and 4 mm ID x 58.5 cm stainless steel fixed-bed down-flow microreactor. The reactor was longer than the furnace which facilitated the placement of the reactor in the furnace by the help of stainless steel fittings. The microreactor was located in the furnace controlled to ± 0.5 K sensitivity by a Shimaden FP-21 programmable temperature controller. Silane treated glass wool was used to hold the catalyst bed in fixed position. The catalyst bed was kept in place by plugging the lower end with silane treated glass wool. The catalyst bed was placed in the center of the reactor which was in the constant-temperature region of the furnace. 20-gauge wire K-type sheathed thermocouple was placed near the center of the catalyst bed just outside the microreactor wall and was connected to the temperature controller. The reactor and furnace system is presented in Figure 4.1. The spaces between the inlet of the reactor-furnace and also the outlet of the reactor-furnace were insulated using ceramic wool to prevent heat loss and maintain stable temperature profile. At the end of the reactor an on-off valve was placed and it was kept closed during feed analysis to prevent back flow of the feed mixture into the reactor.

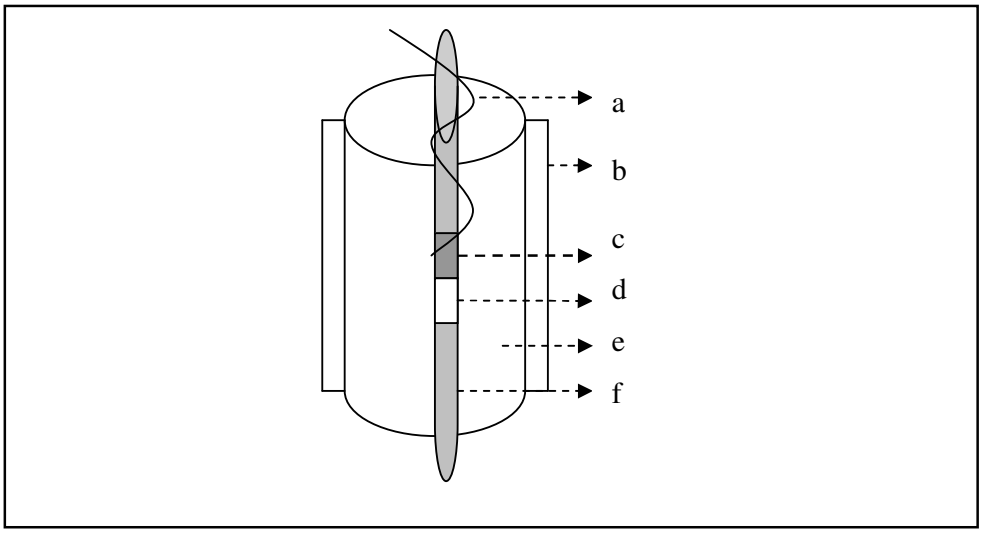

Figure 4.1. Schematic diagram of the reactor and furnace system: a. Thermocouple b. Ceramic wool insulation c. Catalyst d. Catalyst bed e. Furnace f. Reactor

4.1.3. Feed/Product Analysis Section

The product leaving the reactor and the reactant mixtures entering the reactor were analyzed using the gas chromatograph described in Section 3. The product gas stream leaving the microreactor was passed through an on-off valve and sent to the cold trap in order to condense the remaining water vapor before it was sent to the gas chromatograph. Cold trap included a box filled with ice and coiled tubing to increase the contact time between the gas flow and cold environment. The product or reactant gas streams were passed through the three way valve which directed the flow to either the soap bubble flowmeter for measuring the flow rate or to the gas chromatograph for gas analysis. The gases entered the gas chromatograph through a 1/16" stainless steel tube, therefore, the diameter of the stainless steel connecting lines were decreased gradually from 1/4" to 1/8" and 1/16" after the last three way valve. The materials used in the system are listed in Table 4.2 and the system is shown in Figure 4.2.

Table 4.2. Materials and equipment used in the construction of the system

Material and Equipment	Number of Pieces
Two way valve, 1/4"	6
Three way valve, 1/4"	3
Two way connector, 1/4"	6
Two way connector, 1/4" → 1/8"	3
Two way connector, 1/8" → 1/16"	3
Three way connector, 1/4"	4
Three way connector, 1/16"	1
Mass flow controllers	4
Furnace	1
Gas chromatograph	1
Liquid pump	1
Cold trap	1
Temperature controller	2

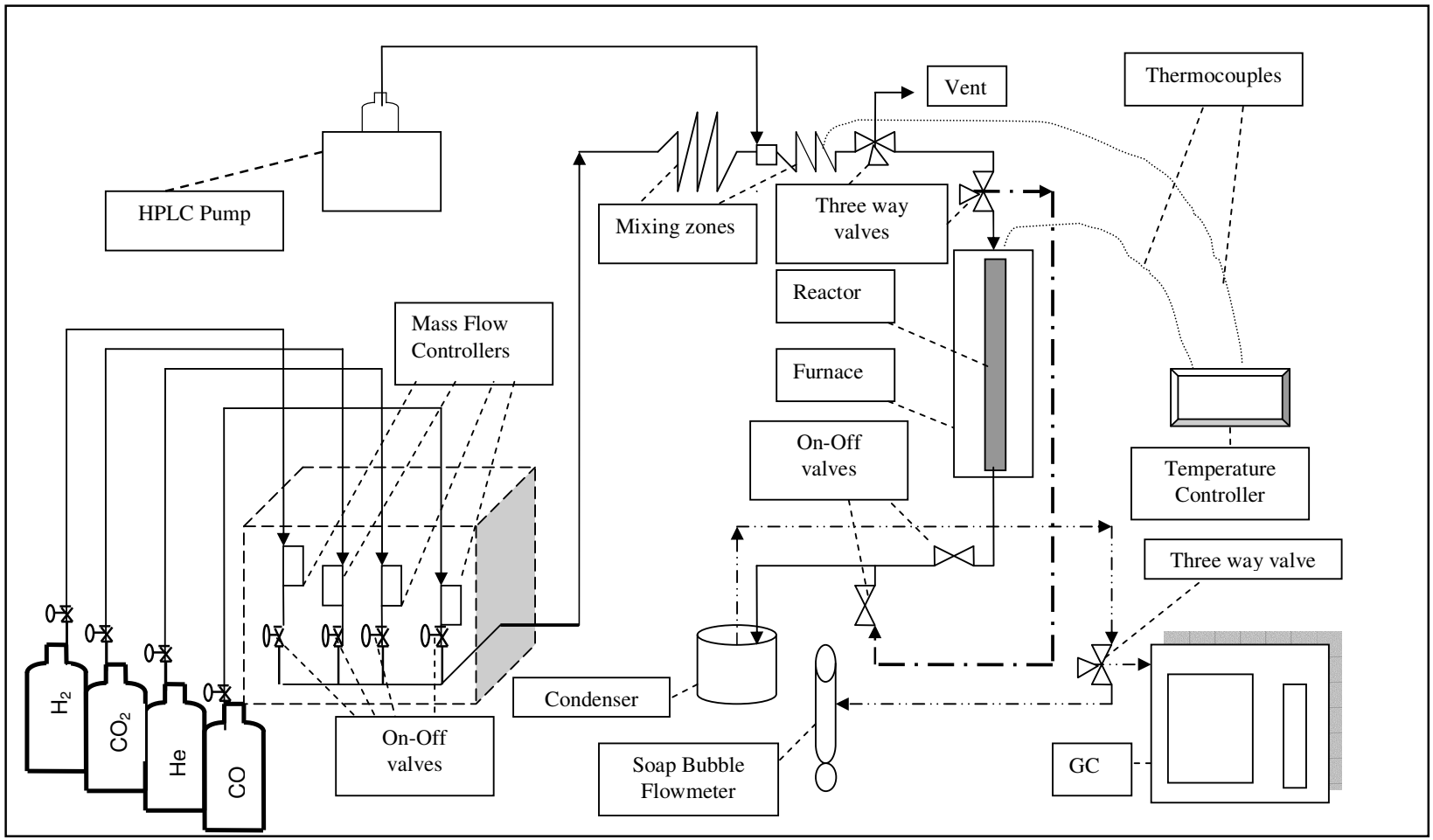

Figure 4.2. The microreactor flow and product analysis system

4.2. Low-Temperature Water-Gas Shift Reaction Experiments

Among the catalysts used for low-temperature water-gas shift reaction, Pt-CeO_x catalysts seem to be the most active according to their good performance in CO conversion and resistance to deactivation (Farias *et al.*, 2007). Alumina is mostly preferred as support material for the noble metal-based catalysts. Therefore, Pt-CeO_x-Al_2O_3 catalysts are cited as promising catalysts for CO clean-up for on-board applications (Quiney *et al.*, 2006).

The purpose of the present study was to construct and test the system suitable for studying the low-temperature water-gas shift reaction. After the design and construction of the system, three Pt-CeO_x/γ-Al_2O_3 catalysts were prepared by changing their cerium oxide content and using sequential impregnation. These catalysts were used in the activity tests.

4.2.1. Parameters of Activity

Catalyst particle size, gas space velocity and contact time are important factors which influence internal and external mass transfer resistances in a heterogeneous system. In previous studies and reactor systems, catalyst particles 250-344 μm in size were found to be sufficiently small to avoid internal mass transport effects arising from pore diffusion under the reaction conditions used (Akın and Önsan, 1997). Therefore, catalyst particle size was chosen between 255-344 μm.

Different parameters were measured in order to see their effects on CO conversion in low-temperature water-gas shift reaction. These parameters were reduction time, residence time (W/F_{CO} ratio), reaction temperature, H_2O/CO ratio and cerium oxide loading. The equilibrium curve for the carbon monoxide conversion was also constructed using a feed composition of 5 per cent CO, 5 per cent H_2O and He as balance. The conversion of CO was defined and calculated as follows:

$$\text{CO conversion } (\%) = \frac{[CO]_{in} - [CO]_{out}}{[CO]_{in}} \times 100 \qquad (4.1)$$

The amount of liquid water used in the experiments was calculated as follows:

$$V_{Steam(H_2O)} = \frac{V_{Liquid(H_2O)} \times \rho_{H_2O} \times R \times T}{MW_{H_2O} \times P} \quad (4.2)$$

where ρ=1000 $g.L^{-1}$; P=1 atm; R=0.082 $L.atm.mol^{-1}.K^{-1}$; T=298 K and MW_{H2O}=18 $g.mol^{-1}$.

The composition of the reactor outlet stream was measured at 30-minute intervals for 3 hours and these data were used for CO conversion calculations. In all experiments, steady state was reached after 60 minutes, as indicated by the CO conversions obtained. The water-gas shift reaction reduces the carbon monoxide concentration in the reformate gas stream of a fuel processor; therefore, CO conversion shapes are the main borders in this work. The amount of hydrogen obtained in the experiments was also presented since another advantage of the water-gas shift reaction is the production of additional hydrogen. The results obtained for all reaction conditions are discussed in the following sections.

4.2.2. Effect of W/F_{CO} Ratio

The first step in the study was to investigate the effect of residence time on the CO conversion. The reactions were carried out at 300°C using a feed gas mixture of 5 per cent CO, 5 per cent H_2O and He as balance. The catalyst used in the experiments at different residence times was 1.4wt.%Pt-10wt.%CeO_x/γ-Al_2O_3. The reduction time was 2 hours. The weight of the catalyst was 250 mg but total flow rates which directly affected the contact time were changed as 100, 150 and 200 $ml.min^{-1}$. CO conversions for different W/F_{CO} ratios are presented in Table 4.3 and Figure 4.3.

In the experiments, 1.4wt.%Pt-10wt.%CeO_x/γ-Al_2O_3 catalyst exhibited relatively high CO conversions at all three W/F_{CO} ratios at 300°C and three hours time-on-stream. At 0.61 $mg.min.\mu mol^{-1}$ residence time, the catalyst exhibited CO conversion values lower than those at the two higher residence times which indicated that CO conversion increases with the W/F_{CO} until 0.81 $mg.min.\mu mol^{-1}$, after which it remains constant since almost complete CO conversion is achieved. These findings coincide well with those of Yeragi *et*

al. (2006), who showed that CO conversion increased as the contact time was increased and space velocity was decreased. Kumar and Idem (2007) reported similar results.

Table 4.3. CO conversion over the 1.4wt.%Pt-10wt.%CeO_x/γ-Al_2O_3 catalyst at different W/F_{CO} ratios at 300°C

Time (min)	W/F_{CO} (mg.min.µmol^{-1})		
	1.22	0.81	0.61
	CO conversion (%)		
30	90.4	84	96.3
60	99	99.4	79
90	98.4	99.2	86
120	99	89.7	83.8
150	98.4	92.4	78.5
180	98	96.4	83

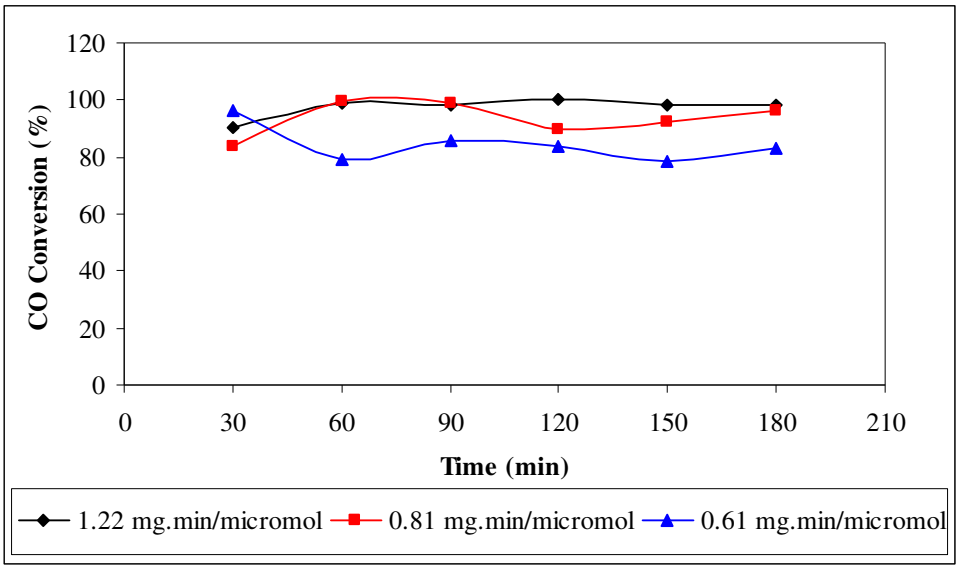

Figure 4.3. Effect of W/F_{CO} ratio on CO conversion over 1.4wt.%Pt-10wt.%CeO_x/γ-Al_2O_3 catalyst at 300°C

The W/F_{CO} ratio was selected as 0.61 mg.min.µmol^{-1} in the following experiments. When the equilibrium conversions of CO with respect to temperature were considered, the conversions exhibited by the catalyst at this residence time were appropriate according to the equilibrium curve. The maximum amount of produced hydrogen is five volume per cent because of the initial composition of the feed gas mixture and according to the stoichiometric balance. Hydrogen amounts were also consistent with the CO conversion values (Figure 4.4).

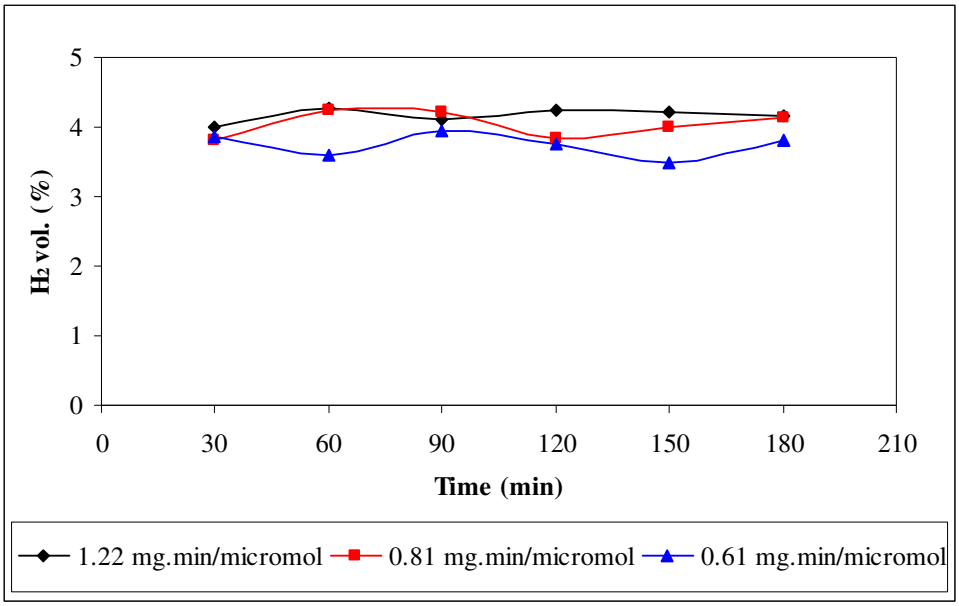

Figure 4.4. Effect of W/F_{CO} ratio on product H_2 (vol.%) over 1.4wt.%Pt-10wt.%CeO_x/γ-Al_2O_3 catalyst at 300°C

4.2.3. Effect of Reduction Time

Secondly, the effect of reduction time on the CO conversion activity of the catalyst was investigated for determining the optimum conditions of the reaction. The experiments were carried out at 300°C using feed gas mixture of 5 per cent CO, 5 per cent H_2O and He as balance. The catalyst used in these experiments was 1.4wt.%Pt-10wt.%CeO_x/γ-Al_2O_3. CO conversion values for reduction times of 2 and 3 hours are presented in Table 4.4 and Figure 4.5.

Table 4.4. CO conversion results for 1.4wt.%Pt-10wt.%CeO_x/γ-Al_2O_3 catalyst at different reduction times

Time (min)	Reduction time (h)	
	2	3
	CO conversion (%)	
30	96.3	69.4
60	79	86.5
90	86	82
120	87	88.6
150	78.5	83.2
180	83	89

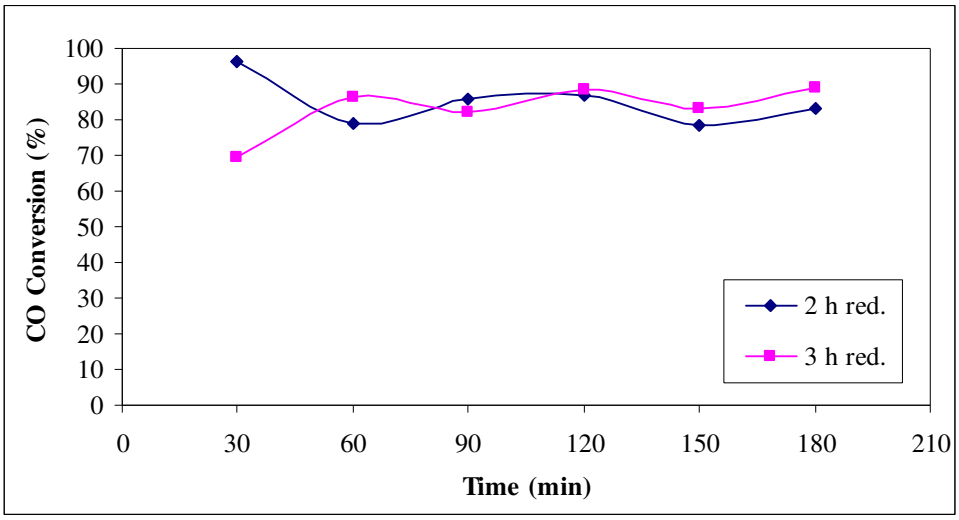

Figure 4.5. Effect of reduction time on CO conversion over 1.4wt.%Pt-10wt.%CeO_x/γ-Al_2O_3 catalyst at 300°C

After the initial sampling at 30 minutes time, steady state was reached at 60 minutes and the catalyst exhibited approximately the same CO conversions for different reduction times. There was no significant effect of reduction time on the CO conversion activity of the catalyst. In the following experiments, 3 hours reduction at 350°C was applied to the catalysts.

4.2.4. Effect of Reaction Temperature

The dependence of CO conversion on the reaction temperature was studied over all three catalysts reduced at 350°C for 3 hours. The composition of the feed gas mixture was 5 per cent CO, 5 per cent H_2O and He as balance. The equilibrium conversions of CO with respect to temperature were also calculated for this feed gas composition. The equilibrium curve giving composition as a function of temperature was determined by using the computer software HSC4 (HSC Chemistry Version 4.1, Outokumpu Research Oy.) and is presented in Figure 4.6. This software uses thermodynamic calculations.

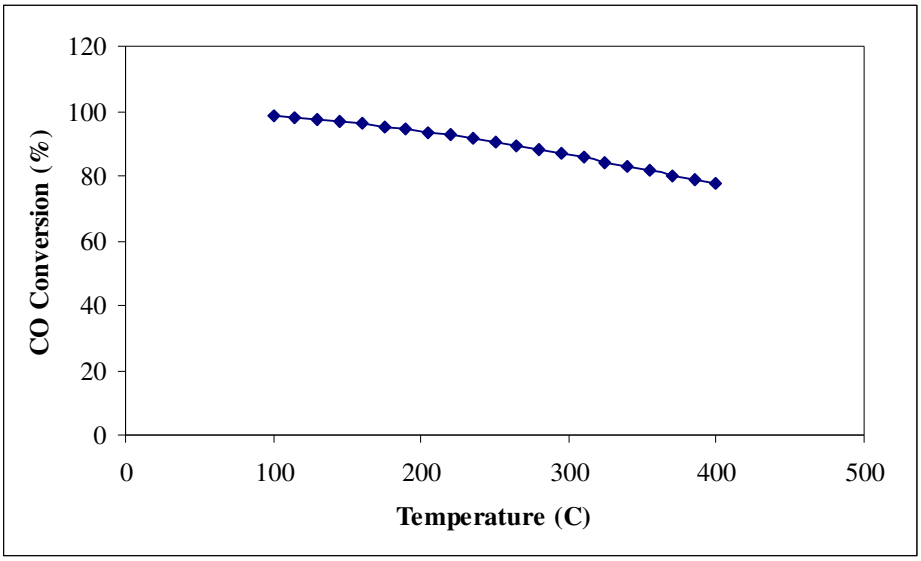

Figure 4.6. Equilibrium curve of the water-gas shift reaction for a feed gas composition of 5% CO and 5% H_2O in He

The water-gas shift reaction is a moderately exothermic reaction. The equilibrium conversion of CO is dependent on the reaction temperature. As seen in Figure 4.6, the CO conversion is higher at lower temperatures, i.e. the equilibrium conversion decreases with increasing temperature, according to Le Chatelier's principle for exothermic reactions, which states that the equilibrium shifts to the left as the temperature increases.

The reaction temperatures studied for seeing their effect on CO conversion were 300, 275 and 250°C for all three catalysts. 1.4wt.%Pt-10wt.%CeO_x/γ-Al_2O_3 catalyst was studied

first. CO conversions obtained are given in Table 4.5 and Figure 4.7 showing the remarkable effect of temperature on catalyst activity. CO conversion increased with increasing temperature since the reaction was not at equilibrium under these conditions.

Table 4.5. CO conversion over 1.4wt.%Pt-10wt.%CeO_x/γ-Al_2O_3 at different reaction temperatures using feed with 5% CO, 5% H_2O in He

Time (min)	CO conversion (%)		
	300°C	275°C	250°C
30	69.4	78.2	34
60	86.5	58.4	36.7
90	82	58	32.1
120	88.6	57.2	28
150	83.2	60.5	31.3
180	89	54.1	11.6

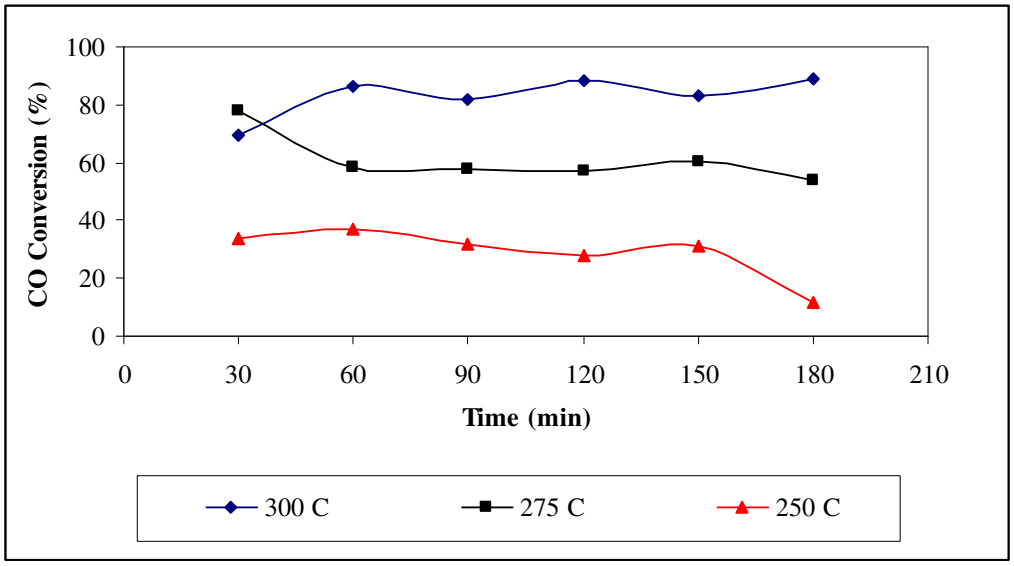

Figure 4.7. Effect of reaction temperature on CO conversion over 1.4wt.%Pt-10wt.%CeO_x/γ-Al_2O_3 catalyst

1.4wt.%Pt-10wt.%CeO_x/γ-Al_2O_3 was also tested at 350°C to investigate the effect of higher temperatures on the behavior of the catalyst in comparison to the equilibrium curve. CO conversions are presented in Table 4.6. CO conversion approached the equilibrium curve when temperature was increased. Further increase in the reaction temperature led to a slight decrease in CO conversion and the trend for the CO conversion resembled the equilibrium curve (Figure 4.8).

Table 4.6. CO conversion over 1.4wt.%Pt-10wt.%CeO_x/γ-Al_2O_3 at different reaction temperatures (90 minutes time-on-stream)

Temperature (°C)	CO conversion (%)
350	81.1
300	82
275	58.1
250	32.1

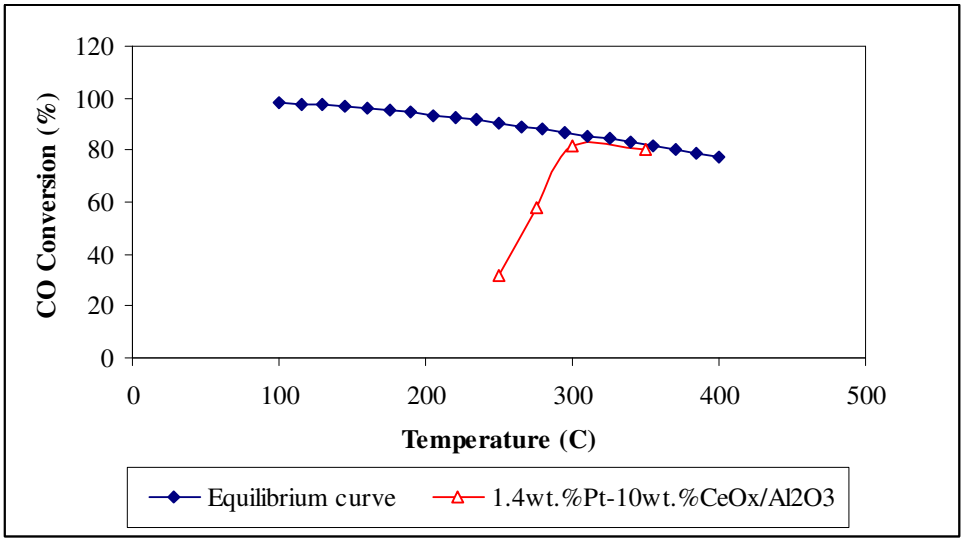

Figure 4.8. CO conversion versus temperature over 1.4wt.%Pt-10wt.%CeO_x/γ-Al_2O_3 with respect to equilibrium (90 minutes time-on-stream)

In the following experiments, the effect of temperature was also studied over 1.4wt.%Pt-5wt.%CeO_x/γ-Al_2O_3 and 1.4wt.%Pt-1.25wt.%CeO_x/γ-Al_2O_3 using the same

feed composition. The CO conversion activities of these catalysts are presented in Tables 4.7, 4.8 and Figures 4.9 and 4.10.

Table 4.7. CO conversion over 1.4wt.%Pt-5wt.%CeO_x/γ-Al_2O_3 at different reaction temperatures using feed with 5% CO, 5% H_2O in He

Time (min)	CO conversion (%)		
	300°C	275°C	250°C
30	86.8	54.6	32.2
60	88.6	55.4	24.3
90	83	58.7	23.8
120	73.1	63.2	24.1
150	85.6	55.5	23
180	83.6	47.5	14.8

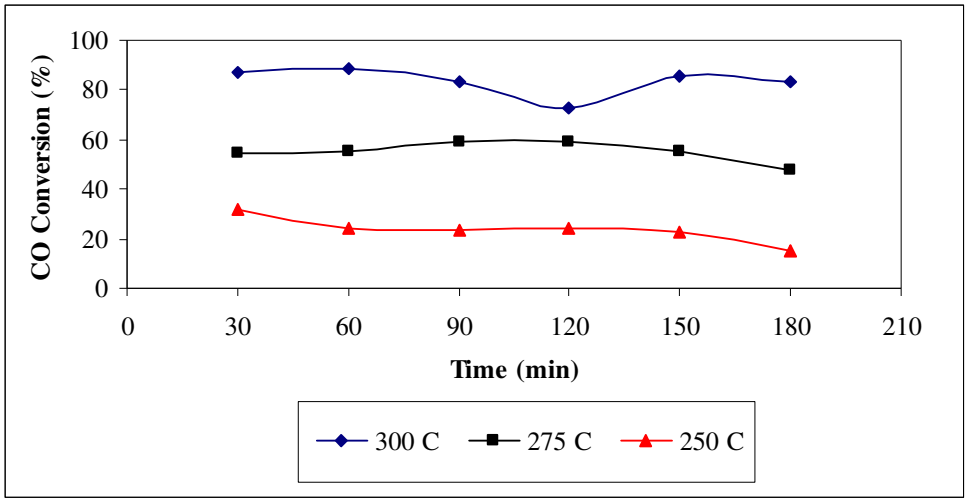

Figure 4.9. Effect of reaction temperature on CO conversion over 1.4wt.%Pt-5wt.%CeO_x/γ-Al_2O_3 catalyst

Table 4.8. CO conversion over 1.4wt.%Pt-1.25wt.%CeO_x/γ-Al_2O_3 at different reaction temperatures using feed with 5% CO, 5% H_2O in He

Time (min)	CO conversion (%)		
	300°C	275°C	250°C
30	70.8	39.2	15.7
60	73.8	34.5	16
90	72.2	28.1	12.7
120	74.6	29.2	11.6
150	70.3	29.1	14
180	69.7	31.4	11

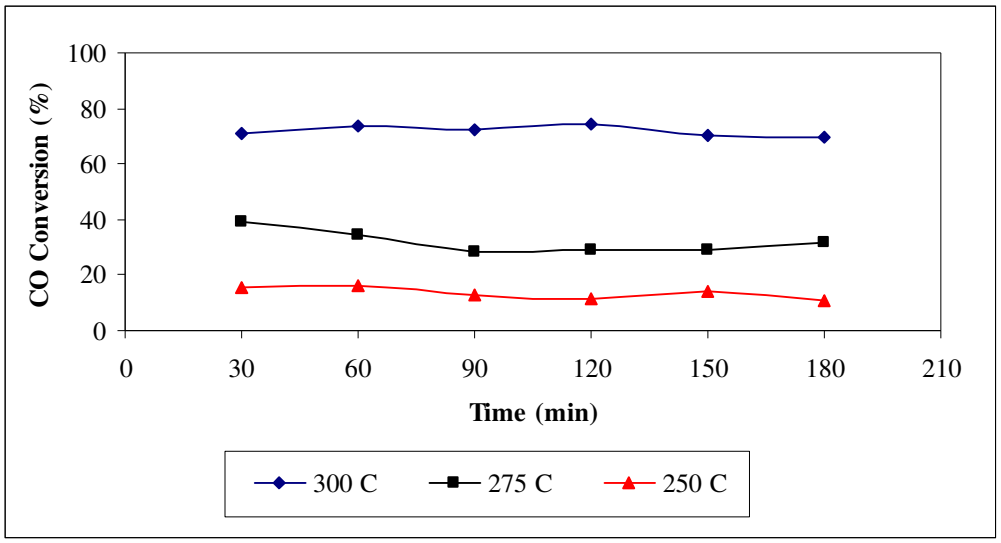

Figure 4.10. Effect of reaction temperature on CO conversion over 1.4wt.%Pt-1.25wt.%CeO_x/γ-Al_2O_3 catalyst

The CO conversions obtained over these catalysts at 90 minutes time-on-stream were plotted under the equilibrium curve (Figures 4.11 and 4.12). Wheeler *et al.* (2004) have reported that the CO conversion activity of Pt/Ceria catalysts reached the equilibrium curve as temperature increased and then exhibited a profile similar to the equilibrium curve.

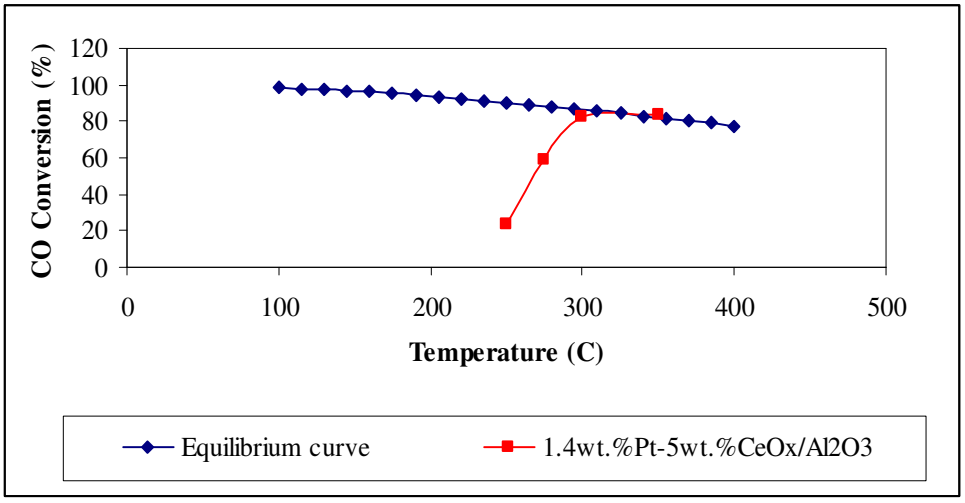

Figure 4.11. CO conversion versus temperature over 1.4wt.%Pt-5wt.%CeO_x/γ-Al_2O_3 with respect to equilibrium (90 minutes time-on-stream)

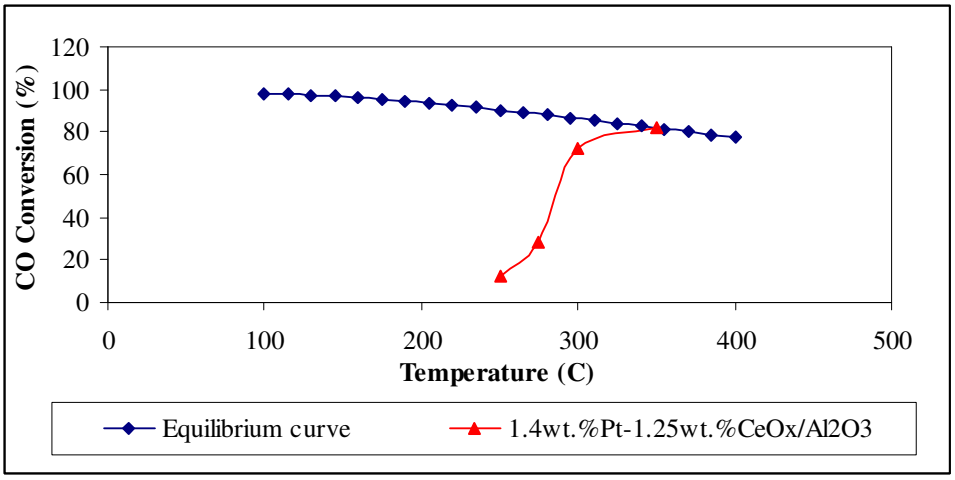

Figure 4.12. CO conversion versus temperature over 1.4wt.%Pt-1.25wt.%CeO_x/γ-Al_2O_3 with respect to equilibrium (90 minutes time-on-stream)

4.2.5. Effect of Cerium Oxide Loading in the Catalysts

The effect of CeO_x content is evident when Figures 4.7-4.12 above are compared. The three catalysts were compared at three different reaction temperatures in order to see the effect of cerium oxide loading on the CO conversion. Again, 5 per cent CO and 5 per

cent H_2O in He balance was used as feed mixture. All catalysts were reduced at 350°C for 3 hours. Tables 4.9 to 4.11 and Figures 4.13 to 4.15 show the CO conversion activities of catalysts having different cerium oxide contents.

Table 4.9. CO conversion over different catalysts at 300°C

Time (min)	CO conversion (%)		
	1.4wt.%Pt-10wt.%CeO_x/γ-Al_2O_3	1.4wt.%Pt-5wt.%CeO_x/γ-Al_2O_3	1.4wt.%Pt-1.25wt.%CeO_x/γ-Al_2O_3
30	69.4	86.8	70.8
60	86.5	88.6	73.8
90	82	83	72.2
120	88.6	73.1	74.6
150	83.2	85.6	70.3
180	89	83.6	69.7

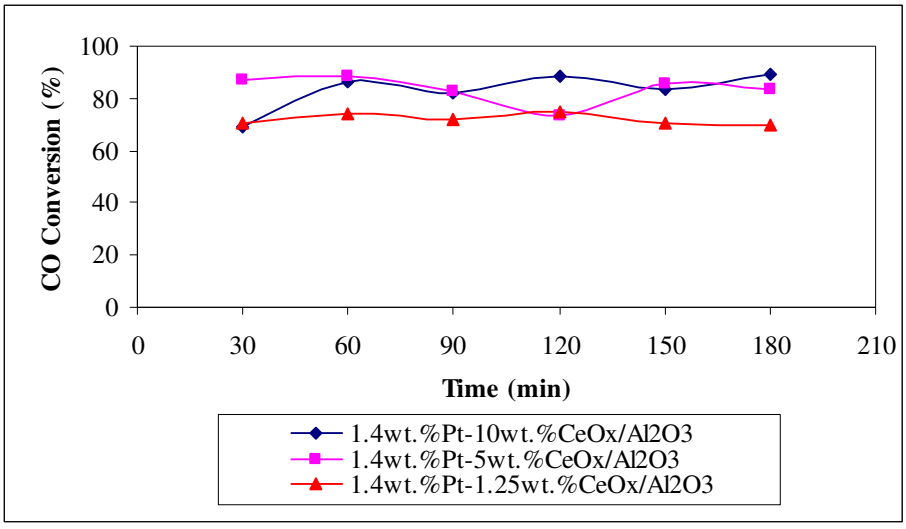

Figure 4.13. Effect of cerium oxide content on CO conversion at 300°C

Catalysts containing 10 weight per cent and 5 weight per cent CeO_x exhibited comparable CO conversions while the 1.4wt.%Pt-1.25wt.%CeO_x/γ-Al_2O_3 catalyst showed relatively lower activity. In addition, this catalyst demonstrated more stable time on stream

profile at 300°C than the other two catalysts. Figures 4.14 and 4.15 demonstrate that the 1.4wt.%Pt-1.25wt.%CeO_x/γ-Al_2O_3 catalyst exhibits CO conversions lower than the other two catalysts at all reaction temperatures. These results indicate that CeO_x loadings above 5 weight per cent are unnecessary, probably because the coverage by CeO_x of the alumina support is almost complete, and loadings between 1.25-5 weight per cent may be tested to determine the optimum CeO_x content required for high CO conversion.

Table 4.10. CO conversion over different catalysts at 275°C

Time (min)	CO conversion (%)		
	1.4wt.%Pt-10wt.%CeO_x/γ-Al_2O_3	1.4wt.%Pt-5wt.%CeO_x/γ-Al_2O_3	1.4wt.%Pt-1.25wt.%CeO_x/γ-Al_2O_3
30	78.2	54.6	39.2
60	58.4	55.4	34.5
90	58	58.7	28.1
120	57.2	63.2	29.2
150	60.5	55.5	29.1
180	54.1	47.5	31.4

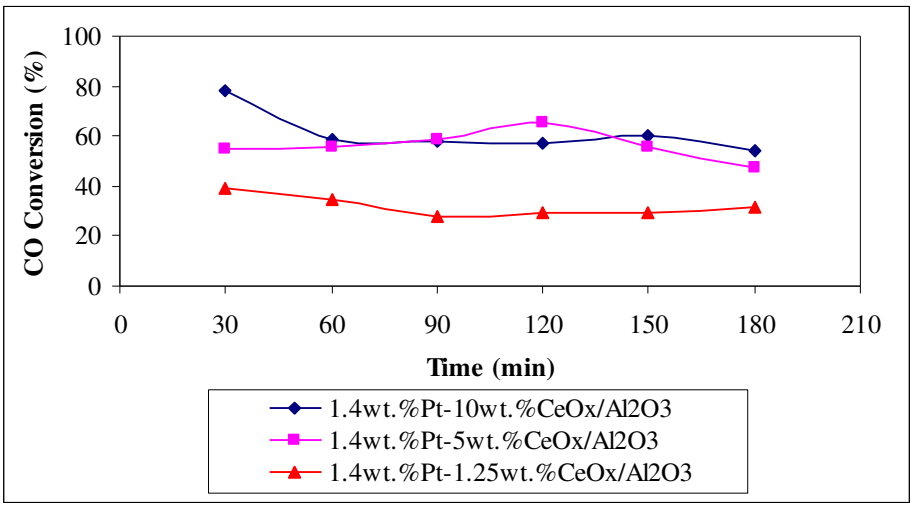

Figure 4.14. Effect of cerium oxide content on CO conversion at 275°C

Table 4.11. CO conversion over different catalysts at 250°C

Time (min)	CO conversion (%)		
	1.4wt.%Pt-10wt.%CeO_x/γ-Al_2O_3	1.4wt.%Pt-5wt.%CeO_x/γ-Al_2O_3	1.4wt.%Pt-1.25wt.%CeO_x/γ-Al_2O_3
30	34	32.2	15.7
60	36.7	24.3	16
90	32.1	23.8	12.7
120	28	24.1	11.6
150	31.3	23	14
180	11.6	14.8	11

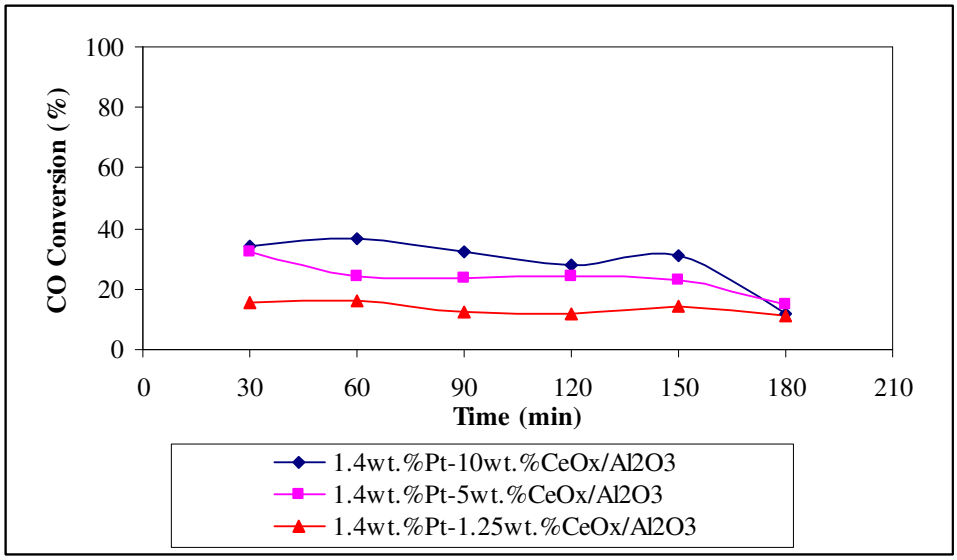

Figure 4.15. Effect of cerium oxide content on CO conversion at 250°C

The hydrogen produced was also examined over the three catalysts and found to be consistent with CO conversions. The results obtained at 300°C are given in Figure 4.16.

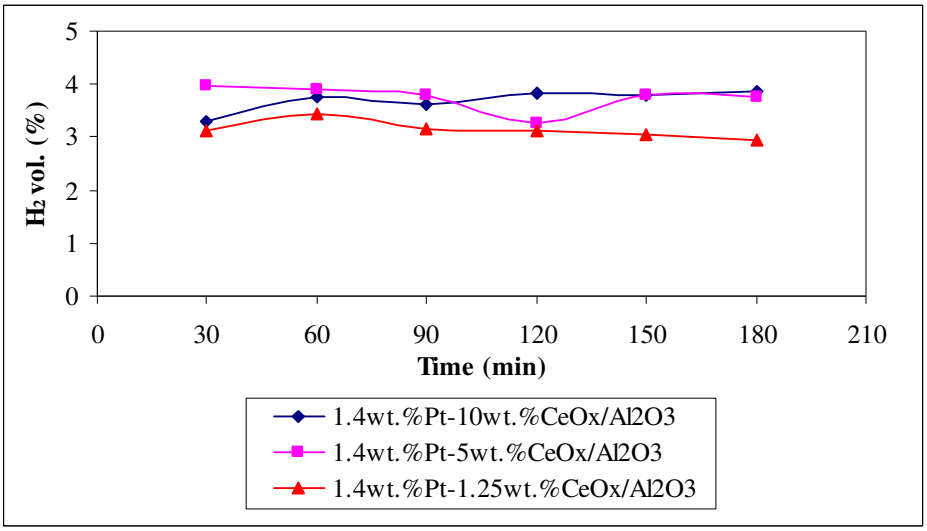

Figure 4.16. Effect of cerium oxide content on H_2 concentration at 300°C

4.2.6. Effect of H_2O/CO Ratio

Since CO conversions obtained at all reaction temperatures were relatively lower over the catalyst with the lowest CeOx content, the dependence of CO conversion on the H_2O/CO molar ratio was investigated at 250°C over 1.4wt.%Pt-1.25wt.%CeO_x/γ-Al_2O_3 in order to be able to observe its effect more clearly. The feed compositions used were 5 per cent CO and 5 per cent H_2O, 5 per cent CO and 10 per cent H_2O, 5 per cent CO and 15 per cent H_2O, in balance He, respectively. Table 4.12 and Figure 4.17 show the CO conversions obtained at different H_2O/CO ratios.

The catalyst exhibited moderately higher CO conversions at H_2O/CO ratio of 3/1. As the ratio was increased from one to three, CO conversion increased, which is in agreement with the study of Andreeva *et al.* (2002) who stated that catalytic activity increased slightly with the H_2O/CO ratio. The effects of H_2O/CO ratio on CO conversion at 250°C are expected to show similar trends for the two other catalysts.

Table 4.12. CO conversion over 1.4wt.%Pt-1.25wt.%CeO_x/γ-Al_2O_3 at different H_2O/CO ratios at 250°C

Time (min)	H_2O/CO ratio		
	1	2	3
	CO conversion (%)		
30	15.7	25.4	34.7
60	16	17.8	29.8
90	12.7	16.8	26.6
120	11.6	13.4	24.8
150	14	10.2	24.4
180	11	12.8	28.2

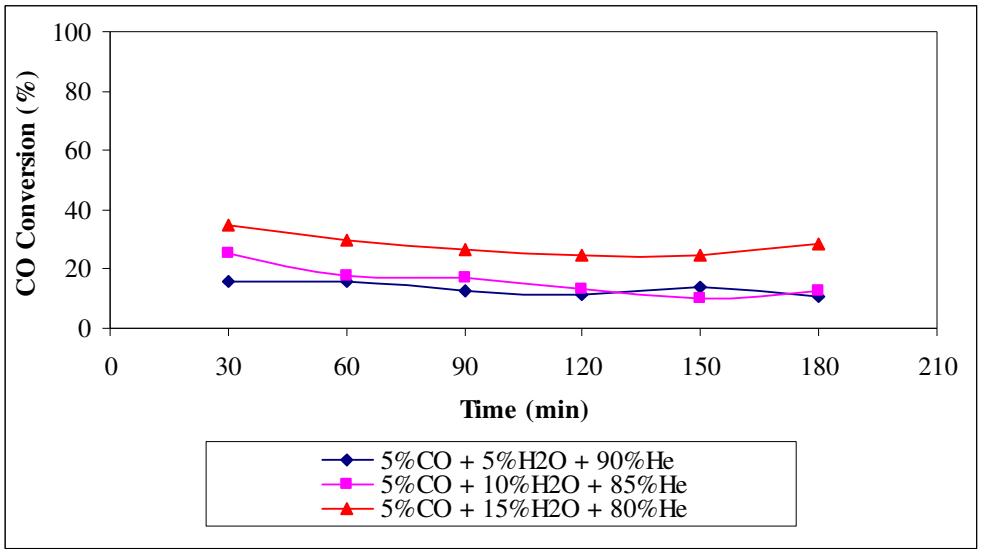

Figure 4.17. Effect of H_2O/CO ratio on CO conversion at 250°C over 1.4wt.%Pt-1.25wt.%CeO_x/γ-Al_2O_3

5. CONCLUSIONS AND RECOMMENDATIONS

5.1. Conclusions

The purpose of this work was to construct and test a low-temperature water-gas shift reaction system. The microreactor flow system was designed and constructed with necessary tubing and fittings and auxiliary units. The testing of the microreactor flow system constructed was carried out using three different catalysts having the same Pt content and different cerium oxide loadings supported on γ-Al_2O_3. All catalysts were prepared by sequential incipient-to-wetness impregnation. Catalyst reduction time, reaction temperature, residence time (W/F_{CO} ratios) and feed composition represented by H_2O/CO ratios were the parameters used to investigate the characteristics of the low-temperature water-gas shift reaction.

The major conclusions obtained in this study can be summarized as follows:

- CO conversion increases with increasing residence time, as indicated by the results obtained over 1.4wt.%Pt-10wt.%CeO_x/γ-Al_2O_3 at 300^{o}C for W/F_{CO} ratios between 0.61-1.22 mg.min.μmol^{-1}.
- Catalyst reduction time has no significant effect on the CO conversion activity of the 1.4wt.%Pt-10wt.%CeO_x/γ-Al_2O_3 catalyst reduced at 350^{o}C under pure hydrogen flow; therefore, a reduction period of three hours can be selected.
- The reaction temperature has considerable effect on CO conversion for all Pt-CeO_x catalysts studied. CO conversion increases as reaction temperature is increased from 250 to 350^{o}C until the limits of the equilibrium curve, further increase in temperature leads to a decrease in CO conversion according to the equilibrium curve of the water-gas shift reaction.
- CO conversion tends to decrease as cerium oxide content of the catalyst decreases. This effect is significant for 1.4wt.%Pt-1.25wt.%CeO_x/γ-Al_2O_3 catalyst while there is no remarkable difference between 1.4wt.%Pt-10wt.%CeO_x/γ-Al_2O_3 and 1.4wt.%Pt-5wt.%CeO_x/γ-Al_2O_3 catalysts. CO conversion activity of 1.4wt.%Pt-1.25wt.%CeO_x/ γ-Al_2O_3 catalyst is found to slightly increase with increasing H_2O/CO ratio.

5.2. Recommendations

Under the light of the results of the present work, the following studies are recommended:

- As indicated by the results of this study, CeO_x loadings higher than 5 weight per cent are not necessary and loadings between 1.25 and 5 weight per cent may be tested to determine the optimum CeO_x content required for obtaining the highest CO conversions.
- Kinetic experiments may be conducted for finding an empirical kinetic expression for low-temperature water-gas shift reaction over the Pt-CeO_x/γ-Al_2O_3 catalyst.
- Physical properties of the three catalysts such as BET surface area, XRD, SEM images may be obtained to study the interaction between Pt and CeO_x components of the Pt-CeO_x/γ-Al_2O_3 catalyst.

APPENDIX A: CALIBRATION CURVES OF THE GAS CHROMATOGRAPH

Calibration curves of the gas chromatograph used in the experiments are given below.

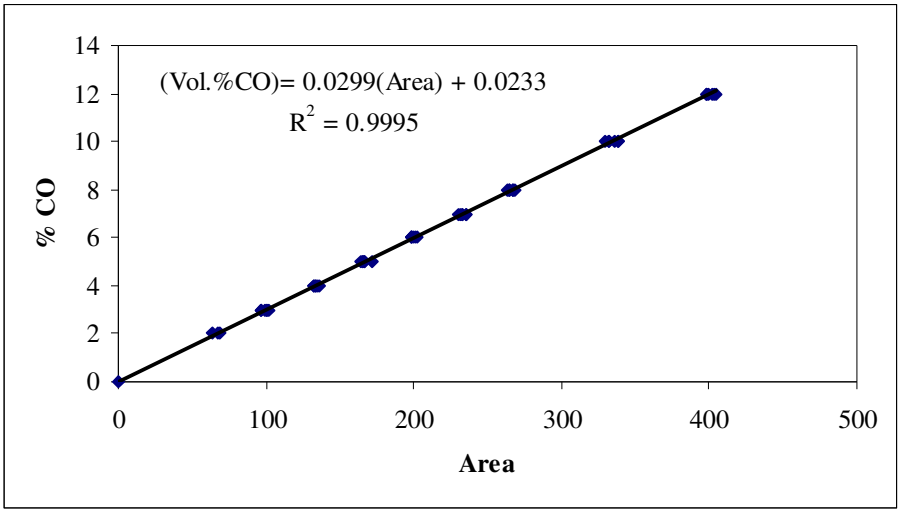

Figure A.1. Calibration curve of carbon monoxide

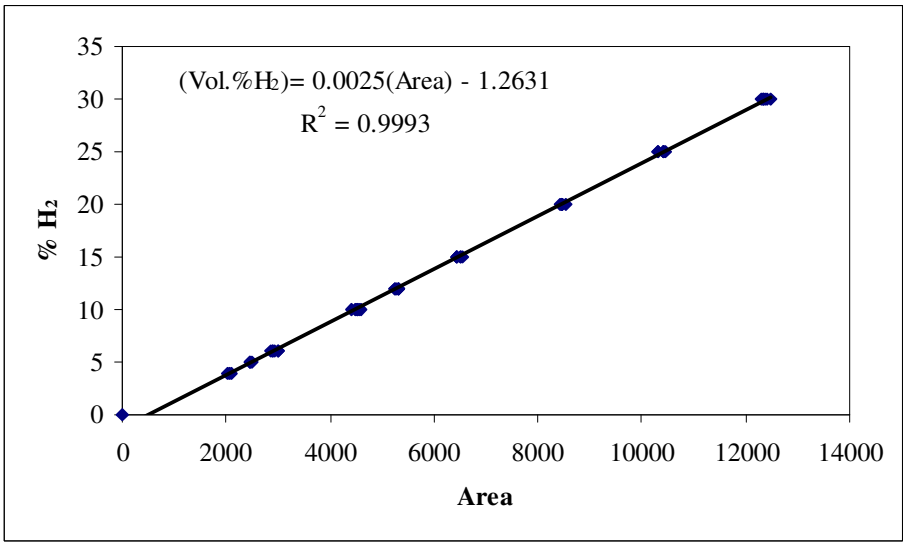

Figure A.2. Calibration curve of hydrogen

APPENDIX B: CALIBRATION CURVES OF THE MASS FLOW CONTROLLERS

Calibration curves of the mass flow controllers used in the experiments are illustrated below.

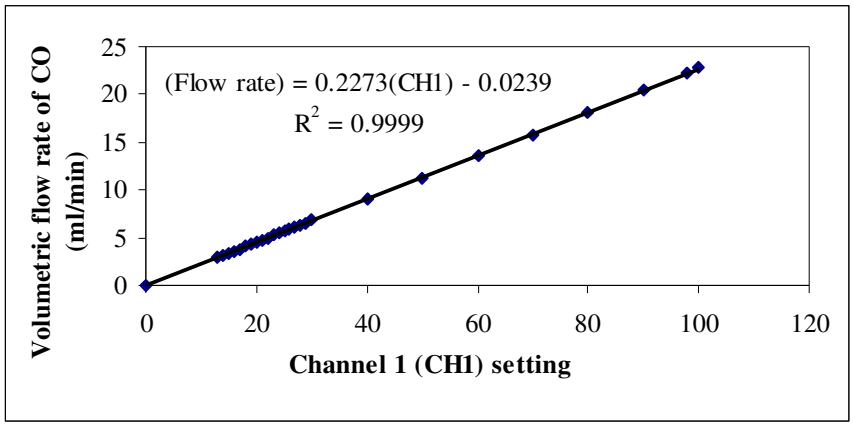

Figure B.1. Calibration curve of the carbon monoxide mass flow controller

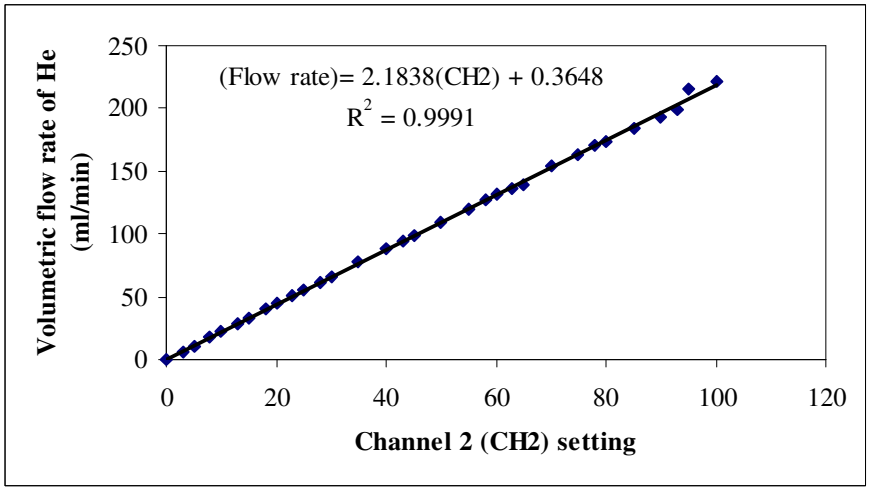

Figure B.2. Calibration curve of the helium mass flow controller

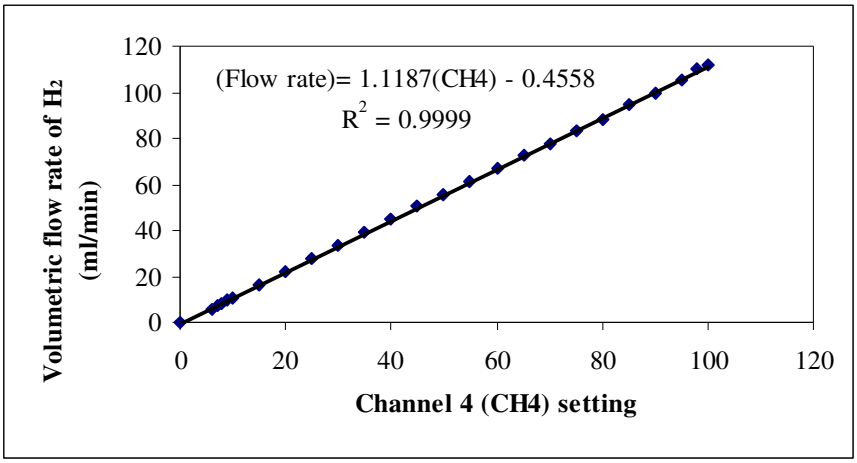

Figure B.3. Calibration curve of the hydrogen mass flow controller

REFERENCES

Adams, W. A., J. Blair, K. R. Bullock and C. L. Gardner, 2005, "Enhancement of the Performance and Reliability of CO Poisoned PEM Fuel Cells", *Journal of Power Sources*, Vol. 145, pp. 55-61.

Ahmed, S. and M. Krumpelt, 2001, "Hydrogen from Hydrocarbon Fuels for Fuel Cells", *International Journal of Hydrogen Energy*, Vol. 26, pp. 291-301.

Akın, A. N., 1996, *Development of Coprecipitated Cobalt-Alumina Catalysts for the Production of C_1-C_4 Hydrocarbons by Carbon Monoxide Hydrogenation*, Ph. D. Dissertation, Boğaziçi University.

Akın, A. N. and Z. İ. Önsan, 1997, "Kinetics of CO Hydrogenation over Coprecipitated Cobalt-Alumina", *Journal of Chemical Technology and Biotechnology*, Vol. 70, pp. 304-310.

Alcaide, F., P. L. Cabot and E. Brillas, 2006, "Fuel Cells for Chemicals and Energy Cogeneration", *Journal of Power Sources*, Vol. 153, pp. 47-60.

Amadeo, N. E. and M. A. Laborde, 1995, "Hydrogen Production from the Low-Temperature Water-Gas Shift Reaction: Kinetics and Simulation of the Industrial Reactor", *International Journal of Hydrogen Energy*, Vol. 20, pp. 949-956.

Anderson, J. R., M. Boudart, 1982, *Catalysis Science and Technology*, Springer-Verlag, Berlin Heidelberg, New York.

Andreeva, D., T. Tabakova, V. Idakiev, P. Christov and R. Giovanoli, 1998, "Au/α-Fe_2O_3 Catalyst for Water-Gas Shift Reaction Prepared by Deposition-Precipitation", *Applied Catalysis A: General*, Vol. 169, pp. 9-14.

Andreeva, D., V. Idakiev, T. Tabakova, L. Ilieva, P. Falaras, A. Bourlinos and A. Travlos, 2002, "Low-Temperature Water-Gas Shift Reaction over Au/CeO_2 Catalysts", *Catalysis Today*, Vol. 72, pp. 51-57.

Andreeva, D., I. Ivanov, L. Ilieva and M. V. Abrashev, 2006, "Gold Catalysts Supported on Ceria and Ceria-Alumina for Water-Gas Shift Reaction", *Applied Catalysis A: General*, Vol. 302, pp. 127-132.

Araujo, G. C. and M. C. Rangel, 2000, "An Environmental Friendly Dopant for the High-Temperature Shift Catalysts", *Catalysis Today*, Vol. 262, pp. 201-207.

Avcı, A. K., Z. İ. Önsan, D. L. Trimm, 2001, "On-Board Fuel Conversion for Hydrogen Fuel Cells : Comparison of Different Fuels by Computer Simulations", *Applied Catalysis A: General*, Vol. 216, pp. 243-256

Avcı, A. K., D. L. Trimm, Z. İ. Önsan, 2002, "Quantitative Investigation of Catalytic Natural Gas Conversion for Hydrogen Fuel Cell Applications", *Chemical Engineering Journal*, Vol. 90, pp. 77-87.

Avcı, A. K., D. L. Trimm, A. E. Aksoylu and Z. İ. Önsan, 2003, "Ignition Characteristics of Pt, Ni, and Pt-Ni Catalysts used for Autothermal Fuel Processing", *Catalysis Letters*, Vol. 88, pp. 17-22..

Azzam, K. G., I. V. Babich, K. Seshan, L. Lefferts, 2007, "A Bifunctional Catalyst for the Single-Stage Water-Gas Shift Reaction in Fuel Cell Applications: Part 2. Roles of the Support and Promoter on Catalyst Activity and Stability", *Journal of Catalysis*, Vol. 251, pp. 163-171.

Basini, L. and L. Piovesan, 1998, "Reduction on Synthesis Gas Costs by Decrease of Steam/Carbon and Oxygen/Carbon Ratios in the Feed Stock", *Industrial and Engineering Chemistry Research*, Vol. 37, pp. 258-266.

Basinska, A. and F. Domka, 1999, "The Effect of Lanthanides on the Ru/Fe_2O_3 Catalysts for Water-Gas Shift Reaction", *Applied Catalysis A: General*, Vol. 179, pp. 241-246.

Boettner, D. D. and M. J. Moran, 2004, "Proton Exchange Membrane (PEM) Fuel Cell-Powered Vehicle Performance Using Direct-Hydrogen Fueling and On-Board Methanol reforming", *Energy*, Vol. 29, pp. 2317-2330.

Brown, L. F., 2001, "A Comparative Study of Fuels for On-Board Hydrogen Production for Fuel-Cell-Powered Automobiles", *International Journal of Hydrogen Energy*, Vol. 26, pp. 381-397.

Bunluesin, T., R. J. Gorte, G. W. Graham, 1998, "Studies of the Water-Gas Shift-Reaction on Ceria-Supported Pt, Pd, and Rh: Implications for Oxygen-Storage Properties", *Applied Catalysis B: Environmental*, Vol. 15, pp. 107-114.

Cheekatamarla, P. K., W. S. Epling and A. M. Lane, 2005, "Selective Low-Temperature Removal of Carbon Monoxide from Hydrogen-Rich Fuels over Cu-Ce-Al Catalysts", *Journal of Power Sources*, Vol. 147, pp. 178-183.

Choi, Y. and H. G. Stenger, 2003, "Water-Gas Shift Reaction Kinetics and Reactor Modeling for Fuel Cell Grade Hydrogen", *Journal of Power Sources*, Vol. 124, pp. 432-439.

Costa, J. L. R., G. S. Marchetti, M. C. Rangel, 2002, "A Thorium-Doped Catalyst for the High Temperature Shift Reaction", *Catalysis Today*, Vol. 77, pp. 205-213.

Denkwitz, Y., A. Karpenko, V. Plzak, R. Leppelt, B. Shumacher and R. J. Behm, 2007, "Influence of CO_2 and H_2 on the Low-Temperature Water-Gas Shift Reaction on Au/CeO_2 Catalysts in Idealized and Realistic Reformate", *Journal of Catalysis*, Vol. 26, pp. 74-90.

Docter, A. and A. Lamm, 1999, "Gasoline Fuel Cell Systems", *Journal of Power Sources*, Vol. 84, pp. 194-200.

Farias, A. M. D., A. P. M. G. Barandas, R. F. Perez and M. A. Fraga, 2007, "Water-Gas Shift Reaction over Magnesia-Modified Pt/CeO_2 Catalysts", *Journal of Power Sources*, Vol. 165, pp. 854-860.

Fiolitakis, E. and H. Hoffman, 1983, "Dependence of the Kinetics of the Low-Temperature Water-Gas Shift Reaction on the Catalyst Oxygen Activity as Investigated by Wavefront Analysis", *Journal of Catalysis*, Vol. 80, pp. 328-339.

Fu, Q., S. Kudriavtseva, H. Saltsburg, M. F. Stephanopoulos, 2003, "Gold-Ceria Catalysts for Low-Temperature Water-Gas Shift Reaction", *Chemical Engineering Journal*, Vol. 93, pp. 41-53.

Fu, Q., W. Deng, H. Saltsburg, M. F.-Stephanopoulos, 2005, "Activity and Stability of Low Content Gold-Cerium Oxide Catalysts for the Water-Gas Shift Reaction", *Applied Catalysis B: Environmental*, Vol. 56, pp. 57-68.

Ghenciu, A. F., 2002, "Review of Fuel Processing Catalysts for Hydrogen Production in PEM Fuel Cell Systems", *Current Opinion in Solid State and Materials Science*, Vol. 6, pp. 389-399.

Goerke, O., P. Pfeifer, K. Schubert, 2004, "Water Gas Shift Reaction and Selective Oxidation of CO in Microreactors", *Applied Catalysis A: General*, Vol. 263, pp. 11-18.

Goguet, A., F. Meunier, J. P. Breen, R. Burch, M. I. Petch and A. F. Ghenciu, 2004, "Study of the Origin of the Deactivation of a Pt/CeO_2 Catalyst during Reverse Water Gas Shift (RWGS) Reaction", *Journal of Catalysis*, Vol. 226, pp. 382-392.

Gorte, R. J., and S. Zhao, 2005, "Studies of the Water-Gas Shift Reaction with Ceria-Supported Precious Metals", *Catalysis Today*, Vol. 104, pp. 18-24.

Harrison, B., A. F. Diwell, C. Hallet, 1988, "Promoting Platinum Metals by Ceria: Metal-Support Interactions in Autocatalysis", *Platinum Metals Review*, Vol. 32, pp. 73-83.

Hilaire, S., X. Wang, T. Luo, R. J. Gorte, J. Wagner, 2001, "A Comparative Study of Water-Gas-Shift Reaction over Ceria Supported Metallic Catalysts", *Applied Catalysis A: General*, Vol. 215, pp. 271-278.

Hua, J., Q. Zheng, Y. Zheng, K. Wei, X. Lin, 2005, "Influence of Modifying Additives on the Catalytic Activity and Stability of Au/Fe_2O_3-MO_x Catalysts for the WGS Reaction", *Catalysis Letters*, Vol. 102, pp. 99-108.

Huber, F., Z. Yu, J. C. Walmsley, D. Chen, H. J. Venvik and A. Holmen, 2007, "Nanocrystalline Cu-Ce-Zr Mixed Oxide Catalysts for Water-Gas Shift: Carbon Nanofibers as Dispersing Agent for the Mixed Oxide Particles", *Applied Catalysis B: Environmental*, Vol. 71, pp. 7-15.

Idakiev, V., T. Tabakova, Z. Y. Yuan, B. L. Su, 2004, "Gold Catalysts Supported on Mesoporous Titania for Low-Temperature Water-Gas Shift Reaction", *Applied Catalysis A: General*, Vol. 270, pp. 135-141.

Idakiev, V., T. Tabakova, A. Naydenov, Z. Y. Yuan, B. L. Su, 2006, "Gold Catalysts Supported on Mesoporous Zirconia for Low-Temperature Water-Gas Shift Reaction", *Applied Catalysis B: Environmental*, Vol. 63, pp. 178-186.

Iida, H. and A. Igarashi, 2006, "Difference in the Reaction Behavior Between Pt-Re/TiO_2 (Rutile) and Pt-Re/ZrO_2 Catalysts for Low-Temperature Water Gas Shift Reactions", *Applied Catalysis A: General*, Vol. 303, pp. 48-55.

Iida, H., K. Kondo, A. Igarashi, 2006, "Effect of Pt Precursors on Catalytic Activity of Pt/TiO_2 (rutile) for Water-Gas Shift Reaction at Low-Temperature", *Catalysis Communications*, Vol. 7, pp. 240-244.

Jacobs, G., L. Williams, U. M. Graham, G. A. Thomas, D. E. Sparks, B. H. Davis, 2003, "Low-Temperature Water-Gas Shift: In Situ DRIFTS-Reaction Study of Ceria Surface Area on the Evolution of Formates on Pt/CeO_2 Fuel Processing Catalysts for Fuel Cell Applications", *Applied Catalysis A: General*, Vol. 252, pp. 107-118.

Jacobs, G., P. M. Patterson, L. Williams, E. Chenu, D. Sparks, G. Thomas and B. H. Davis, 2004, "Water-Gas Shift: In Situ Spectroscopic Studies of Noble Metal Promoted Ceria Catalysts for CO Removal in Fuel Cell Reformers and Mechanistic Implications", *Applied Catalysis A: General*, Vol. 262, pp. 177-187.

Jacobs, G., P. M. Patterson, U. M. Graham, A. C. Crawford, A. Dozier and B. H. Davis, 2005a, "Catalytic Links among the Water-Gas Shift, Water-Assisted Formic Acid Decomposition, and Methanol Steam Reforming Reactions over Pt-Promoted Thoria", *Journal of Catalysis*, Vol. 235, pp. 79-91.

Jacobs, G., U. M. Graham, E. Chenu, P. M. Patterson, A. Dozier and B. H. Davis, 2005b, "Low-Temperature Water-Gas Shift: Impact of Pt Promoter Loading on the Partial Reduction of Ceria and Consequences for Catalyst Design", *Journal of Catalysis*, Vol. 229, pp. 499-512.

Jacobs, G., S. Ricote, B. H. Davis, 2006, "Low Temperature Water-Gas Shift: Type and Loading of Metal Impacts Decomposition and Hydrogen Exchange Rates of Pseudo-Stabilized Formate over Metal-Ceria Catalysts", *Applied Catalysis A: General*, Vol. 302, pp. 14-21.

Keiski, R. L., O. Desponds, Y. F. Chang and G. A. Somorjai, 1993, "Kinetics of the Water-Gas Shift Reaction over Several Alkane Activation and Water-Gas Shift Catalysts", *Applied Catalysis A: General*, Vol. 101, pp. 317-338.

Kim, C. H. and L. T. Thompson, 2005, "Deactivation of Au/CeO_x Water Gas Shift Catalysts", *Journal of Catalysis*, Vol. 230, pp. 66-74.

Koeppel, R. A., A. Baiker, C. Shild, A. Wokaun, 1991, "Carbon Dioxide Hydrogenation over Au/ZrO_2 Catalysts from Amorphous Precursors: Catalytic Reaction Mechanism", *Journal of the Chemical Society, Faraday Transactions*, Vol. 87, pp. 2821-2828.

Koryabkina, N. A., A. A. Phatak, W. F. Ruettinger, R. J. Farrauto, F. H. Ribeiro, 2003, "Determination of Kinetic Parameters for the Water-Gas Shift Reaction on Copper Catalysts under Realistic Conditions for Fuel Cell Applications", *Journal of Catalysis*, Vol. 217, pp. 233-239.

Krumpelt, M., T. R. Krause, J. D. Carter, J. P. Kopasz, S. Ahmed, 2002, "Fuel Processing for Fuel Cell Systems in Transportation and Portable power Applications", *Catalysis Today*, Vol. 77, pp. 3-16.

Kumar, P. and R. Idem, 2007, "A Comparative Study of Copper-Promoted Water-Gas Shift (WGS) Catalysts", *Energy & Fuels*, Vol. 21, pp. 522-529.

Kusar, H., S. Hocevar, J. Levec, 2006, "Kinetics of the Water-Gas Shift Reaction over Nanostructured Copper-Ceria Catalysts", *Applied Catalysis B: Environmental*, Vol. 63, pp. 194-200.

Laniecki, M., M. M. Grycz, F. Domka, 2000, "Water-Gas Shift Reaction over Sulfided Molybdenum Catalysts I. Alumina, Titania, and Zirconia-Supported Catalysts", *Applied Catalysis A: General*, Vol. 196, pp. 293-303.

Lei, Y., N. W. Cant, D. L. Trimm, 2005a, "Activity Patterns for the Water Gas Shift Reaction over Supported Precious Metal Catalysts", *Catalysis Letters*, Vol. 103, pp. 133-136.

Lei, Y., N. W. Cant, D. L. Trimm, 2005b, "Kinetics of the Water-Gas Shift Reaction over a Rhodium-Promoted Iron-Chromium Oxide Catalyst", *Chemical Engineering Journal*, Vol. 114, pp. 81-85.

Lei, Y., N. W. Cant, D. L. Trimm, 2006, "The Origin of Rhodium Promotion of Fe_3O_4-Cr_2O_3 Catalysts for the High-Temperature Water-Gas Shift Reaction", *Journal of Catalysis*, Vol. 239, pp. 227-236.

Leppelt, R., B. Schumacher, V. Plzak, M. Kinne, R. J. Behm, 2006, "Kinetics and Mechanism of the Low-Temperature Water-Gas Shift Reaction on Au/CeO_2 Catalysts in an Idealized Reaction Atmosphere", *Journal of Catalysis*, Vol. 244, pp. 137-152.

Li, Y., Q. Fu, M. F.-Stephanopoulos, 2000, "Low-Temperature Water-Gas Shift Reaction over Cu- and Ni-Loaded Cerium Oxide Catalysts", *Applied Catalysis B: Environmental*, Vol. 27, pp. 179-191.

Litster, S. and G. Mclean, 2004, "PEM Fuel Cell Electrodes", *Journal of Power Sources*, Vol. 130, pp. 61-76.

Liu, Q., W. Ma, R. He, Z. Mu, 2005a, "Reaction and Characterization Studies of an Industrial Cr-free Iron-Based Catalyst for High Temperature Water Gas Shift Reaction", *Catalysis Today*, Vol. 106, pp. 52-56.

Liu, X., W. Ruettinger, X. Xu, R. Farrauto, 2005b, "Deactivation of Pt/CeO_2 Water-Gas Shift Catalysts due to Shut Down, Startup Modes for Fuel Cell Applications", *Applied Catalysis B: Environmental*, Vol. 56, pp. 69-75.

Luengnaruemitchai, A., S. Osuwan, E. Gulari, 2003, "Comparative Studies of Low-Temperature Water-Gas Shift Reaction over Pt/CeO_2, Au/CeO_2 and Au/Fe_2O_3 Catalysts", *Catalysis Communications*, Vol. 4, pp. 215-221.

Mendelovici, L. and M. Steinberg, 1985, "Methanation and Water-Gas Shift Reactions over Pt/CeO_2", *Journal of Catalysis*, Vol. 96, pp. 285-287.

Nagai, M., A. M. Zahidul, K. Matsuda, 2006, "Nano-Structured Nickel-Molybdenum Carbide Catalyst for Low-Temperature Water-Gas Shift Reaction", *Applied Catalysis A: General*, Vol. 313, pp. 137-145.

Nagai, M. and K. Matsuda, 2006, "Low-Temperature Water-Gas Shift Reaction over Cobalt-Molybdenum Carbide Catalyst", *Journal of Catalysis*, Vol. 238, pp. 489-496.

Natesakhawat, S., X. Wang, L. Zhang, U. S. Ozkan, 2006, "Development of Chromium-Free Iron-Based Catalysts for High-Temperature Water-Gas Shift Reaction", *Journal of Molecular Catalysis A: Chemical*, Vol. 260, pp. 82-94.

Ovesen, C. V., B. S. Clausen, B. S. Hammershoi, G. Steffensen, T. Askgaard, I. Chorkendorff, J. K. Norskov, P. B. Rasmussen, P. Stoltze and P. Taylor, 1996, "A Microkinetic Analysis of the Water-Gas Shift Reaction Under Industrial Conditions", *Journal of Catalysis*, Vol. 158, pp. 170-180.

Panagiotopoulou, P. and D. I. Kondarides, 2004, "Effect of Morphological Characteristics of TiO_2-Supported Noble Metal Catalysts on Their Activity for the Water-Gas Shift Reaction", *Journal of Catalysis*, Vol. 225, pp. 327-336.

Panagiotopoulou, P., A. Christodoulakis, D. I. Kondarides and S. Boghosian, 2006, "Particle Size Effects on the Reducibility of Titanium Dioxide and Its Relation to the Water-Gas Shift Activity of Pt/TiO_2 Catalysts", *Journal of Catalysis*, Vol. 240, pp. 114-125.

Patel, S. and K. K. Pant, 2006, "Activity and Stability Enhancement of Copper-Alumina Catalysts Using Cerium and Zinc Promoters for the Selective Production of Hydrogen Via Steam Reforming of Methanol", *Journal of Power Sources*, Vol. 159, pp. 139-143.

Pintar, A., J. Batista, S. Hocevar, 2007, "Nanostructured $Cu_xCe_{1-x}O_{2-y}$ Mixed Oxide Catalysts: Characterization and WGS Activity Tests", *Journal of Colloidal and Interface Science*, Vol. 307, pp. 145-157.

Quiney, A. S., G. Germani, Y. Schuurman, 2006, "Optimization of a Water-Gas Shift Reactor over a Pt/ceria/Alumina Monolith", *Journal of Power Sources*, Vol. 160, pp. 1163-1169.

Radhakrishnan, R., R. R. Willigan, Z. Dardas, T. H. Vanderspurt, 2006, "Water Gas Shift Activity and Kinetics of Pt/Re Catalysts Supported on Ceria-Zirconia Oxides", *Applied Catalysis B: Environmental*, Vol. 66, pp. 23-28.

Rhodes, C., B. P. Williams, F. King, G. J. Hutchings, 2002, "Promotion of Fe_3O_4/Cr_2O_3 High Temperature Water Gas Shift Catalyst", *Catalysis Communications*, Vol. 3, pp. 381-384.

Ricote, S., G. Jacobs, M. Milling, Y. Ji, P. M. Patterson, B. H. Davis, 2006, "Low-Temperature Water-Gas Shift: Characterization and Testing of Binary Mixed Oxides of Ceria and Zirconia Promoted with Pt", *Applied Catalysis A: General*, Vol. 303, pp. 35-47.

Ruettinger, W., O. Ilinich, R. J. Farrauto, 2003, "A New Generation of Water Gas Shift Catalysts for Fuel Cell Applications", *Journal of Power Sources*, Vol. 118, pp. 61-65.

Ruettinger, W., X. Liu, R. J. Farrauto, 2006, "Mechanism of Aging for a Pt/CeO_2-ZrO_2 Water Gas Shift Catalyst", *Applied Catalysis B: Environmental*, Vol. 65, pp. 135-141.

Saito, M., K. Tomoda, I. Takahara, K. Murata, M. Inaba, 2003, "Effects of Pretreatments of Cu/ZnO-Based Catalysts on Their Activities for the Water-Gas Shift Reaction", *Catalysis Letters*, Vol. 89, pp. 11-13.

Saito, M. and K. Murata, 2004, "Development of High Performance Cu/ZnO-Based Catalysts for Methanol Synthesis and the Water-Gas Shift Reaction", *Catalysis Surveys from Asia*, Vol. 8, pp. 285-294.

Sakurai, H., T. Akita, S. Tsubota, M. Kiuchi, M. Haruta, 2005, "Low-Temperature Activity of Au/CeO_2 for Water-Gas Shift Reaction, and Characterization by ADF-STEM, Temperature-Programmed Reaction, and Pulse Reaction", *Applied Catalysis A: General*, Vol. 291, pp. 179-187.

Scherer, G. G., 1997, "Interfacial Aspects in the Development of Polymer Electrolyte Fuel Cells", *Solid State Ionics*, Vol. 94, pp. 249-257.

Sedmak, G., S. Hocevar, J. Levec, 2004, "Transient Kinetic Model of CO Oxidation over a Nanostructured $Cu_{0.1}Ce_{0.9}O_{2-y}$ Catalyst", *Journal of Catalysis*, Vol. 222, pp. 87-99.

Shido, T. and Y. Iwasawa, 1993, "Reactant-Promoted Reaction Mechanism for Water-Gas Shift Reaction on Rh-Doped CeO_2", *Journal of Catalysis*, Vol. 141, pp. 71-81.

Shishido, T., M. Yamamoto, D. Li, Y. Tian, H. Morioka, M. Honda, T. Sano, K. Takehira, 2006a, "Water-Gas Shift Reaction over Cu/ZnO and Cu/ZnO/Al_2O_3 Catalysts Prepared by Homogeneous Precipitation", *Applied Catalysis A: General*, Vol. 303, pp. 62-71.

Shishido, T., M. Yamamoto, I. Atake, D. Li, Y. Tian, H. Morioka, M. Honda, T. Sano, K. Takehira, 2006b, "Cu/Zn-Based Catalysts Improved by Adding Magnesium for Water-Gas Shift Reaction", *Journal of Molecular Catalysis A: Chemical*, Vol. 253, pp. 270-278.

Son, I. H. and A. M. Lane, 2001, "Promotion of Pt/γ-Al_2O_3 by Ce for Preferential Oxidation of CO in H_2", *Catalysis Letters*, Vol. 76, pp. 151-154.

Son, I. H., 2006, "Study of Ce-Pt/γ-Al_2O_3 for the Selective Oxidation of CO in H_2 for Application to PEFCs: Effect of Gases", *Journal of Power Sources*, Vol. 159, pp. 1266-1273.

Song, C., 2002, "Fuel Processing for Low-Temperature and High-Temperature Fuel Cells: Challenges and Opportunities for Sustainable Development in the 21st Century", *Catalysis Today*, Vol. 77, pp. 17-49.

Tabakova, T., V. Idakiev, D. Andreeva, I. Mitov, 2000, "Influence of the Microscopic Properties of the Support on the Catalytic Activity of Au/ZnO, Au/ZrO_2, Au/Fe_2O_3, Au/Fe_2O_3-ZnO, Au/Fe_2O_3-ZrO_2 Catalysts for the WGS Reaction", *Applied Catalysis A: General*, Vol. 202, pp. 91-97.

Tabakova, T., F. Boccuzzi, M. Manzoli, J. W. Sobczak, V. Idakiev, D. Andreeva, 2004, "Effect of Synthesis Procedure on the Low-Temperature WGS Activity of Au/ceria Catalysts", *Applied Catalysis B: Environmental*, Vol. 49, pp. 73-81.

Tabakova, T., F. Boccuzzi, M. Manzoli, J. W. Sobczak, V. Idakiev, D. Andreeva, 2006, "A Comparative Study of Nanosized IB/ceria Catalysts for Low-Temperature Water-Gas Shift Reaction", *Applied Catalysis A: General*, Vol. 298, pp. 127-143.

Tanaka, Y., T. Utaka, R. Kikuchi, K. Sasaki, K. Eguchi, 2003a, "CO Removal from Reformed Fuel over Cu/ZnO/Al_2O_3 Catalysts Prepared by Impregnation and Coprecipitation Methods", *Applied Catalysis A: General*, Vol. 238, pp. 11-18.

Tanaka, Y., T. Utaka, R. Kikuchi, K. Sasaki, K. Eguchi, 2003b, "Water-Gas Shift Reaction over Cu-Based Mixed Oxides for CO Removal from the Reformed Fuels", *Applied Catalysis A: General*, Vol. 242, pp. 287-295.

Tibiletti, D., F. C. Meunier, A. Goguet, D. Reid, R. Burch, M. Boaro, M. Vicaro, A. Trovarelli, 2006, "An Investigation of Possible Mechanisms for the Water-Gas Shift Reaction over a ZrO_2-Supported Pt Catalyst", *Journal of Catalysis*, Vol. 244, pp. 183-191.

Trimm, D. L. and Z. İ. Önsan, 2001, "Onboard Fuel Conversion for Hydrogen-Fuel-Cell-Driven Vehicles", *Catalysis Reviews-Science and Engineering*, Vol. 43 (1-2), pp. 31-84.

Trimm, D. L., 2005, "Minimisation of Carbon Monoxide in a Hydrogen Stream for Fuel Cell Applications", *Applied Catalysis A: General*, Vol. 296, pp. 1-11.

Trovarelli, A., 1996, "Catalytic Properties of Ceria and CeO_2-Containing Materials", *Catalysis Reviews*, Vol. 38, pp. 439-520.

Utaka, T., T. Okanishi, T. Takeguchi, R. Kikuchi and K. Eguchi, 2003, "Water-Gas Shift Reaction of Reformed Fuel over Supported Ru Catalysts", *Applied Catalysis A: General*, Vol. 245, pp. 343-351.

Velu, S., M. P. Kapoor, S. Inagaki, K. Suzuki, 2003, "Vapor Phase Hydrogenation of Phenol over Palladium Supported on Mesoporous CeO_2 and ZrO_2", *Applied Catalysis A: General*, Vol. 245, pp.317-331.

Venugopal, A., J. Aluha, D. Mogano, M. S. Scurrell, 2003, "The Gold-Ruthenium-Iron Oxide Catalytic System for the Low Temperature Water-Gas-Shift Reaction: The Examination of Gold-Ruthenium Interactions", *Applied Catalysis A: General*, Vol. 245, pp. 149-158.

Wang, X. and R. J. Gorte, 2003, "The Effect of Fe and Other Promoters on the Activity of Pd/ceria for the Water-Gas Shift Reaction", *Applied Catalysis A: General*, Vol. 247, pp. 157-162.

Wen, W., L. Jing, M. G. White, N. Marinkovic, J. C. Hanson and J. A. Rodriguez, 2007, "In Situ Time-Resolved Characterization of Novel Cu-MoO_2 Catalysts during the Water-Gas Shift Reaction", *Catalysis Letters*, Vol. 113, pp. 1-6.

Wheeler, C., A. Jhalani, E. J. Klein, S. Tummala and L. D. Schmidt, 2004, "The Water-Gas-Shift Reaction at Short Contact Times", *Journal of Catalysis*, Vol. 223, pp. 191-199.

Wild, P. J. and M. J. F. M. Verhaak, 2000, "Catalitic Production of Hydrogen from Methanol", *Catalysis Today*, Vol. 60, pp. 3-10.

Yahiro, H., K. Murawaki, K. Saiki, T. Yamamoto and H. Yamaura, 2007, "Study on the Supported Cu-Based Catalysts for the Low-Temperature Water-Gas Shift Reaction", *Catalysis Today*, Vol. 126, pp. 436-440.

Yeragi, D. C., N. C. Pradhan, A. K. Dalai, 2006, "Low-Temperature Water-Gas Shift Reaction over Mn-Promoted Cu/Al_2O_3 Catalysts", *Catalysis Letters*, Vol. 112, pp. 139-148.

Zalc, J. M. and D. G. Löffler, 2002, "Fuel Processing for PEM Fuel Cells: Transport and Kinetic Issues of System Design", *Journal of Power Sources*, Vol. 111, pp. 58-64.

Zalc, J. M., V. Sokolovskii and D. G. Löffler, 2002, "Are Noble Metal-Based Water-Gas Shift Catalysts Practical for Automotive Fuel Processing?", *Journal of Catalysis*, Vol. 206, pp. 169-171.

Zerva, C. and C. J. Philippopoulos, 2006, "Ceria Catalysts for Water Gas Shift Reaction: Influence of Preparation Method on Their Activity", *Applied Catalysis B: Environmental*, Vol. 67, pp. 105-112.